The oxidative demethylation of toluene with bismuth uranate

THE OXIDATIVE DEMETHYLATION OF TOLUENE WITH BISMUTH URANATE

J. G. Steenhof de Jong

THE OXIDATIVE DEMETHYLATION OF TOLUENE WITH BISMUTH URANATE

THE OXIDATIVE DEMETHYLATION OF TOLUENE WITH BISMUTH URANATE

PROEFSCHRIFT

ter verkrijging van de graad van doctor in de technische wetenschappen aan de Technische Hogeschool Eindhoven, op gezag van de rector magnificus, prof.dr.ir. G. Vossers, voor een commissie aangewezen door het college van dekanen in het openbaar te verdedigen op dinsdag 12 december 1972 te 16.00 uur

door

Jacob Gerrit Steenhof de Jong

geboren te Wierden (O)

Druk: Offsetdrukkerij Biblo b.v., 's-Hertogenbosch

DIT PROEFSCHRIFT IS GOEDGEKEURD DOOR DE PROMOTOREN:

Prof.Drs.H.S.van der Baan

Prof.Dr.G.C.A.Schuit

ter herinnering aan mijn vader
aan mijn moeder

CONTENTS

Curriculum vitae

The author was born on september 3rd, 1945, at Wierden (Ov.). After finishing 'gymnasium beta' (secondary school) at Oegstgeest, he started studying chemistry at the University of Leiden in 1963, passed the 'candidaatsexamen' (B.Sc.) in 1966 and the 'doctoraalexamen' (M.Sc.) with subjects organic chemistry (Prof. Dr. E.C. Kooyman), chemical technology (Prof. Drs. P.J. van den Berg of the Delft technical University) and heterogeneous catalysis (Prof. Dr. W.M.H. Sachtler) in 1969. Between 1968 and 1969 he was 'student-assistent' at the laboratory of organic chemistry, in charge of destillation and gas chromatography apparatus. In december 1969 he was appointed 'wetenschappelijk medewerker' (research assistent) at the laboratory of chemical technology of the Eindhoven University.

Acknowledgements

Thanks are due to all who contributed to the present work, in particular to the undergraduates Messrs. L.A. Haak, P.G.F. Lacroix, M.G.M. Steijns and P.A.A. Stolwijk, and to Mr. C.H.E. Guffens, who collaborated in this work for almost two years and played an important role in the realisation of both the experimental and the theoretical parts. Discussions with my colleagues and with Mr. Ph.A. Batist also were of great value. Finally, I am indebted to Miss J.M. van den Heuvel for typing the manuscript, and to Mr. R.J.M. van der Weij for the illustrations.

CHAPTER 1

INTRODUCTION

1.1 The oxidation of toluene

The oxidation of toluene has been the subject of numerous investigations during the last eighty years. This work has resulted in two industrial processes: the oxidation in the liquid phase, usually catalysed by cobalt salts, to form benzoic acid, and the vapour phase oxidation to form benzaldehyde and benzoic acid.

For the latter reaction various metal oxide catalysts are mentioned in literature. Depending on the catalyst composition and the reaction conditions, a great number of by-products are obtained, including maleic, phtalic and citraconic anhydrides, phenol, cresoles, benzoquinone, toluquinone, anthraquinone, benzene, acetic acid and o-methyldiphenylmethane. Also, considerable amounts of CO and CO_2 are formed.

Some of the more recent literature has been summarized in table I.

Table I. CATALYTIC VAPOUR PHASE OXIDATION OF TOLUENE

Author	Catalyst	Conditions	Results	Ref.
Downie	V_2O_5	300-350°	At 20% conversion selectivity in benzaldehyde 60%, in benzoic acid 5%, in maleic anhydride 3%.	(1)
Germain	V_2O_5	450°	At 10% conversion selectivity in benzaldehyde 57%, in benzoic acid 6%.	(2)
	MoO_3	450°	At 10% conversion selectivity in benzaldehyde 64%.	
Reddy	MoO_3/WO_3	500°	At 5% conversion selectivity in benzaldehyde 75%.	(3)
Popova	$CuO/MoO_3/WO_3$	350-450°	At 6% conversion selectivity in benzaldehyde up to 85%.	(4)
Kumar	SnO_2/V_2O_5	300°	At 30% conversion selectivity in benzoic acid 50%, in benzaldehyde 7%.	(5)

It is far less known that toluene can be converted into benzene by oxidation. In 1890, Vincent (6) studied the reaction between toluene and lead oxide. Below 335°, benzene was the main reaction product, the oxide being reduced to metallic lead. Much later Norton and Moss (7) described a process in which toluene was oxidized by air over a cadmium oxide catalyst. However, in our laboratory Heynen (8) found that this catalyst is unsuitable for continuous operation since it is partly reduced to the metal. At the reaction temperature, metallic cadmium has an appreciable vapour pressure, leading to a loss of catalyst during the process. Recently, Adams (9) obtained benzaldehyde and benzene in almost equal yields (16%) using a bismuth molybdate catalyst.

It is rather surprising that the oxidative demethylation reaction has not been studied in more detail, since it could offer an interesting alternative to the hydrodemethylation process which is applied on such a large scale in the petroleum industry; in 1966, 1.2 million tons of benzene were produced from toluene (10).

As far as the costs of the raw materials are concerned, the reaction:

$$C_7H_8 + 1\tfrac{1}{2}\ O_2 \longrightarrow C_6H_6 + CO_2 + H_2O$$

is more attractive than the reaction:

$$C_7H_8 + H_2 \longrightarrow C_6H_6 + CH_4$$

The proceeds of the methane produced (0.5 ¢/Nm^3) are much lower than the costs of the hydrogen used (5 ¢/Nm^3). However, since the yields of the hydrodemethylation process are of the order of 95%, an oxidative route must be very selective in order to be competitive.

1.2 The reaction between toluene and bismuth uranate

In 1971 (11), we described a new reaction to convert toluene into benzene. Toluene is passed over bismuth uranate in a stream of an inert gas at 400-500°. Bismuth uranate acts as an oxidant, and benzene is formed in selectivities up to 70%. The reduced bismuth uranate is reoxidized with air in a separate operation. A continuous process, in which a toluene/air mixture is passed over bismuth uranate does not give satisfactory results, since most of the toluene undergoes total combustion.

1.3 Survey of the present investigation

In this thesis a detailed description of the reaction between toluene and bismuth uranate is given.

Chapter 2 deals with the preparation and properties of various bismuth uranates. Since the compound Bi_2UO_6 seems to be the active component for the title reaction, special attention is paid to its physical properties.

The apparatus used is described in chapter 3.

In chapter 4 a qualitative reaction model is proposed. The reaction end products are determined and the thermodynamic equilibrium is calculated.

The reaction kinetics are described in chapter 5. It appears that the diffusion of oxygen through the lattice of Bi_2UO_6 plays an important role. A model for gas-solid reactions which proceed according to a chemical-reaction plus diffusion mechanism is derived and compared with the experimental results. The diffusion coefficient of two types of lattice oxygen is determined.

In chapter 6 a reaction mechanism is proposed. The reaction between possible intermediates and bismuth uranate, giving additional support to the mechanism, is described.

Finally, in chapter 7 the catalytic activity of a number of other catalyst systems for the oxidation of toluene is reported. Especially with bismuth phosphates promising results are obtained.

Parts of this thesis have been published before (11, 12).

REFERENCES

1. Downie, J., Shelstad, K.A., and Graydon, W.F., *Can.J.Chem. Eng.* 39, 201 (1961).
2. Germain, J.E., and Laugier, R., *Bull.* 1971 (2), 650.
3. Reddy, K.A., and Doraiswamy, L.K., *Chem.Eng.Sci.* 24, 1415 (1969).
4. Popova, N.I., and Kabakova, B.V., *Kin. and Catal.* 5, 289 (1964).
5. Kumar, R.N., Bhat, G.N., Kuloor, N.R., *Indian Chem.Engr.* 7 (4), 78 (1965).
6. Vincent, M.C., *Bull.* 3 4, 6 (1890).
7. Norton, C.J., and Moss, T.E., *U.S.P.* 3,175,016 (1965), *I & EC, Process Design Develop.* 3 (1) 23 (1964).
8. Heynen, H.W.G., private communication (1970).
9. Adams, C.R., *J.Catal.* 10, 355 (1968).
10. *Chemical Economics Handbook*, Stanford Research Institute, Menlo Park, 1972.
11. de Jong, J.G., and Batist, Ph.A., *Rec.trav.Chim.* 90, 749 (1971).
12. Steenhof de Jong, J.G., Guffens, C.H.E., and van der Baan, H.S., *J.Catal.* 26, 401 (1972).

CHAPTER 2

PREPARATION AND PROPERTIES OF BISMUTH URANATES

2.1 Introduction

Literature on the mixed oxides of bismuth and uranium is rather scarce . In 1889, Fischel (1) prepared a red compound by heating bismuth trichloride and uranyl hydroxide together, and gave it the formula $2Bi_2O_3 \cdot 3UO_3$. Berman (2) described a mineral uranosphaerite, with the formula $Bi_2O_3 \cdot 2UO_3 \cdot 3H_2O$ that decomposes upon heating. The system bismuth oxide - uranium oxide was examined in more detail by Erfurth (3) and Hund (4). Their results are summarized in table 2-1.

Table 2-1. THE SYSTEM BISMUTH OXIDE - URANIUM OXIDE

Preparation Method	Formula	Uranium Valency	Bi/U Atomic Ratio	Colour	Structure	a	c	Ref.
From Bi_2O_3 and U_3O_8 in air at 980°.	Bi_2UO_6	6	2/1	Brickred	Hexagonal	7.92[6]	19.53[2]	(3)
	Continuous range to:							
	$Bi_2UO_6 \cdot 0.95Bi_2O_3$	6	3.9/1	Brown	Hexagonal	7.89	19.65	
	$Bi_2UO_6 \cdot Bi_2O_3$	6	4/1	Brown	Cubic	5.64[5]		
	Continuous range to:							
	$Bi_2UO_6 \cdot 5Bi_2O_3$	6	12/1	Dark brown	Cubic	5.60[1]		
	$Bi_2UO_6 \cdot 7Bi_2O_3$	6	16/1	Yellow-brown	Tetragonal	5.50[6]	5.66[2]	
	Continuous range to:							
	$Bi_2UO_6 \cdot 18Bi_2O_3$	6	38/1	Yellow-brown	Tetragonal	5.48[5]	5.66[0]	
From Bi_2O_3 and an equimolar mixture of UO_2 and U_3O_8 in an evacuated tube at 1100°.	$BiUO_4$	5	1/1	Black	Fluorite-type	5.48[1]		(3)
	Continuous range to:							
From $BiUO_4$ and an equimolar mixture of UO_2 and U_3O_8 in an evacuated tube at 1100°.	$BiUO_4 \cdot U_2O_5$	5	1/3	Black	Fluorite-type	5.45[2]		
	Continuous range to:							
	U_2O_5	5		Black	Fluorite-type	5.43[9]		
From UO_2 and Bi_2O_3 under N_2 at 1000°.	Continuous range between UO_2 and δ-Bi_2O_3							
	UO_2	4		Black	Fluorite-type	5.466		(4)
	$Bi_2O_3 \cdot 8UO_2$	4	1/4	Red-brown	Fluorite-type	5.466		
	$Bi_2O_3 \cdot 2UO_2$	4	1/1	Red-brown	Fluorite-type	5.483		
	$Bi_2O_3 \cdot UO_2$	4	2/1	Red-brown	Fluorite-type	5.570		
	$4.5Bi_2O_3 \cdot UO_2$	4	9/1	Brown	Fluorite-type	5.620		
	δ-Bi_2O_3			Yellow	Fluorite-type	5.600*		

* extrapolated

All samples were prepared by prolonged heating of a mixture of the oxides of bismuth and uranium at 800-1100°. Products, obtained this way, have a low specific surface area, and for that reason exhibit a low activity in heterogeneous catalysis and in heterogeneous chemical reactions.

In order to obtain bismuth uranates with a high surface area, we adopted the low-temperature method, described by Batist et al. (5) for the preparation of bismuth molybdate. In this method, nearly colloidal precipitates of the two metal hydroxides are heated together in water at 100°. After drying and calcination a solid is obtained with a high surface area.

2.2 Preparation

Bismuth nitrate or basic nitrate is dissolved in warm, dilute HNO_3. The solution is added to an excess of warm, concentrated ammonia. The white precipitate, consisting of $Bi_2O_3 \cdot xNO_3 \cdot yH_2O$ (6) is filtered off and thoroughly washed with water. A corresponding quantity of uranyl acetate or nitrate is dissolved in warm water and the solution is added to an excess of ammonia. The yellow precipitate, $UO_3 \cdot xNH_3 \cdot yH_2O$ (7) is filtered off and washed with water. Both precipitates should be kept under water to prevent the formation of clots. The two precipitates are transferred to a round-bottomed flask with water, and heated at 90-100° under vigorous stirring. After a few hours, the original yellow colour turns into orange and the gel properties disappear. Apparently a reaction between the two compounds takes place, either directly in the solid phase, or between dissolved uranic acid and bismuth hydroxide.

After 20 hours of stirring, the solid mass is filtered off, washed with water and dried for 20 hours at 135°. Finally, the product is calcined in air at 500° for 1 hour to obtain almost quantitatively a brown, amorphous material.

Thermogravimetrical analysis of the dried, but uncalcined product, carried out in an air atmosphere, reveals a loss of weight in two temperature regions: below 500°, attributed to dehydration, and above 900°, where oxygen is liberated.

Simultaneous differential thermal analysis shows that the process of calcination is exothermic. Since the dehydration should be endothermic, it follows that, apart from the loss of water, another reaction takes place. This is most probably a reaction between the oxides not yet completely converted into bismuth uranate during the boiling process.

In the DTA no definite peaks due to phase transitions were observed . Calcined samples, subjected to DTA, exhibited no endothermic or exothermic effects.

The bismuth uranates, obtained by the method described above, will from now on be referred to as the low-temperature uranates.

We also prepared samples of Bi_2UO_6 and $Bi_2UO_6 \cdot Bi_2O_3$ directly from the oxides after the method of Erfurth. Bismuth oxide and U_3O_8 were thoroughly ground and mixed, and heated in a platinum crucible at 800°. The colour of the mixture rapidly turned into red. Each 24 hours the product was ground again and an aliquot was taken for X-ray examination. After one week no more changes in X-ray pattern were observed. Thereafter, the samples were heated at 1000° for two weeks and slowly cooled to room temperature. In the discussion below these bismuth uranates will be called the high temperature samples.

2.3 Physical properties

Some physical properties of fourteen low-temperature bismuth uranates with different Bi/U atomic ratios are given in table 2-2. Specific surface areas were measured according to the BET-method, using nitrogen as the adsorbate.

We tried to determine the melting points of these compounds under a microscope. A maximum temperature of 1500° was attained. Below this temperature, only bismuth oxide and the samples with Bi/U=3 and 4 melted. Melting points were 830° for the bismuth oxide and 1300° for the bismuth uranates. These measurements, however, were inaccurate, since thermogravimetrical analysis revealed that all bismuth uranates lose oxygen above 900°.

Table 2-2. PROPERTIES OF LOW-TEMPERATURE BISMUTH URANATES

Bi/U atomic ratio	Colour	Specific Surface Area ($m^2.g^{-1}$)
Bismuth oxide	light-yellow	1.3
4/1	ochre	11.4
3/1	brown	25.3
2.33/1	brown	30.0
2/1	brown	22.4
1.86/1	orange-brown	23.4
1.5/1	orange-brown	41.5
1.22/1	orange	15.3
1/1	orange	48.2
1/1.22	orange	27.8
1/1.5	orange	30.4
1/1.86	olive	23.9
1/2.33	olive	26.4
Uranium oxide	orange	25.0

2.4 X-ray diagrams

X-ray diffraction diagrams were measured with a Philips diffractometer, using Ni-filtered Cu-radiation. The spectra of the low-temperature samples consisted of broad, diffuse lines, unsuitable for accurate examination. By heating the samples, the lines narrowed and a characteristic pattern arose. This crystallisation process was followed in a Guinier camera with temperature programming. The results, obtained with a sample Bi/U=2, are given in figure 2-1. It can be seen that most of the line-narrowing occurs up to 700°. Therefore, small parts of our low-temperature samples were calcined for 1 hour at 700°. X-ray diffraction data of these samples are given in figure 2-2.

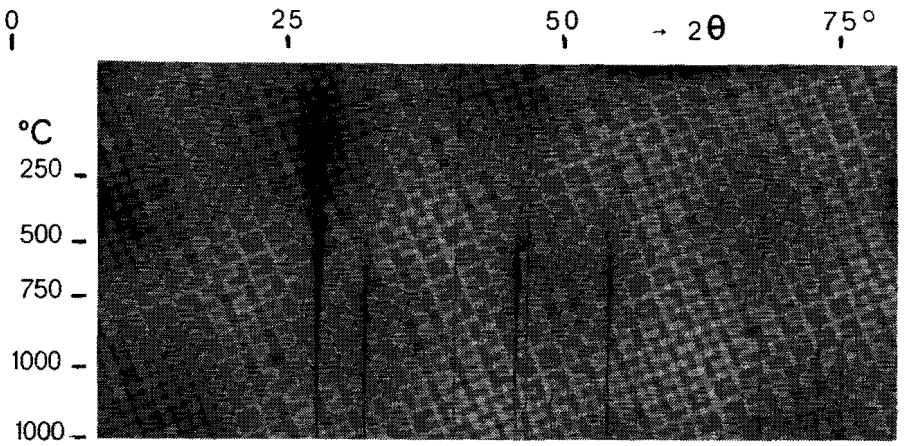

Fig. 2-1 CRYSTALLISATION OF BISMUTH URANATE

(Guinier photograph made at the Reactor Centrum Nederland at Petten)

Our bismuth oxide proves to consist of several modifications, while the uranium oxide, the colour of which had turned to green during the 700°-treatment, is in the U_3O_8-form. The X-ray patterns of the low-temperature sample with Bi/U=2 and that of the high-temperature Bi_2UO_6 are identical and also agree with the diagram given by Erfurth. The conclusion can be drawn that our low-temperature Bi/U=2 sample actually is the compound Bi_2UO_6.

In the samples with Bi/U lower than 2, α-UO_3 is present together with Bi_2UO_6. This is rather surprising, since pure α-UO_3 decomposes at 600° to form U_3O_8 (8), while our samples had been heated at 700°. Probably the Bi_2UO_6-surrounding has a stabilizing influence on α-UO_3, which may be caused by a similarity in crystal structure between α-UO_3 and Bi_2UO_6.

Samples with a Bi/U atomic ratio between 2 and 4, show only lines of Bi_2UO_6. Apparently, a solid solution of Bi_2O_3 in Bi_2UO_6 is present. This is also in agreement with the results of Erfurth. At Bi/U=4, a line pattern appears which is identical with that of high-temperature $Bi_2UO_6 \cdot Bi_2O_3$. However, both diagrams differ from that given by Erfurth, indicating that the crystal structure of our sample is different from the simple cubic structure of Erfurth.

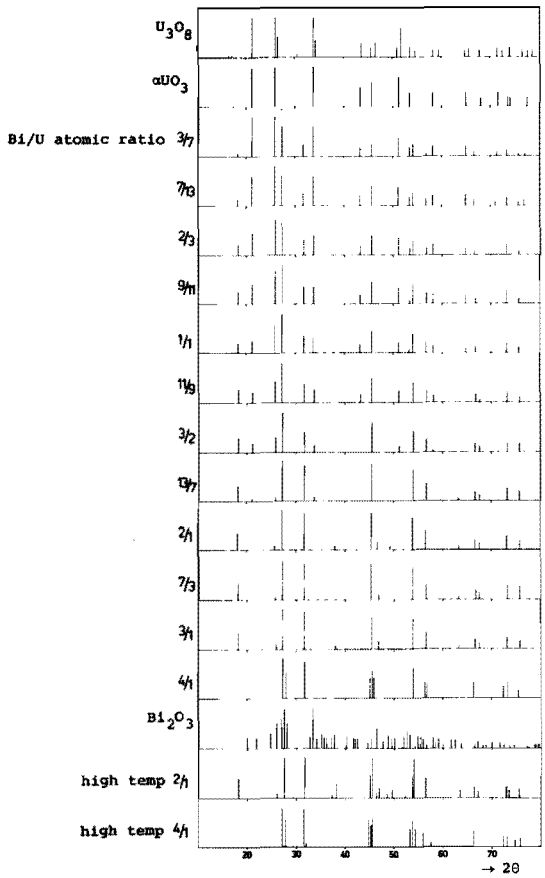

Fig. 2-2 X-ray diffraction data of bismuth uranates

From these results the conclusion can be drawn that, apart from the degree of crystallinity, there is no structural difference between the samples, prepared at low temperatures from the hydroxides, and those, obtained by heating the oxides together at high temperatures.

2.5 Activity in toluene oxidation

The activities of the different bismuth uranates in the reaction with toluene were compared in the pulse system, described in chapter 3. The reactor was filled with a quantity of bismuth uranate corresponding to a surface area of 10 m^2. The reaction conditions were: temperature 480°, pulse volume 0.534 cm^3, toluene/nitrogen molar ratio: 0.077, gas flow 25 $cm^3 . min^{-1}$. In figure 2-3 the maximum selectivities in benzene and productivities are plotted against the Bi/U atomic ratio. Some experiments were also carried out at 450°, but at this temperature the selectivities for all samples were considerably lower than at 480°. It is noted that pure uranium oxide is not only an unselective, but also a very active oxidant. At 400° the toluene was completely converted to CO_2 and H_2O.

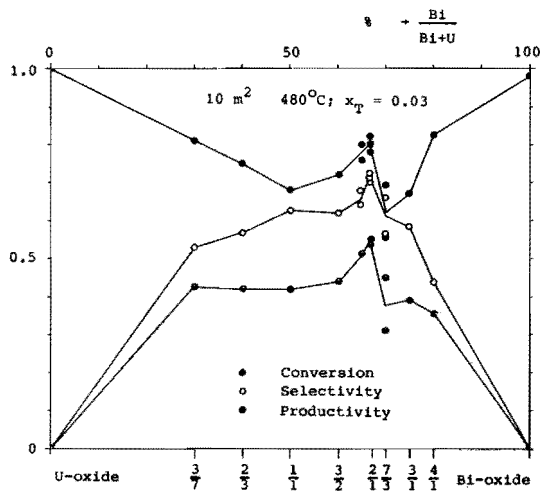

Fig. 2-3 Maximum selectivities and corresponding conversions and productivities as a function of the composition of the bismuth uranate; pulse system

It can be seen from figure 2-3 that both the selectivity and the productivity have a sharp maximum at Bi/U=2. This leads to the conclusion that the active component for the oxidation of toluene to benzene is the compound Bi_2UO_6.

Since the samples on the uranium-rich side of the system consists of Bi_2UO_6 and α-UO_3, the former being the selective, and the latter one the unselective component, it should be possible to improve the selectivities by removing the α-UO_3. For this purpose we used the carbonate leaching process described by Forward and Halpern (9). Uranium oxide is dissolved according to the equation:

$$UO_3 + CO_3^{2-} + 2HCO_3^- \rightarrow UO_2(CO_3)_3^{4-} + H_2O$$

A few grams of bismuth uranate with Bi/U=1/1.86 were added to a solution of 10 g sodium carbonate and 10 g of sodium bicarbonate in 100 ml of water, and boiled for 1 hour. The solution turned yellow. The solid was filtered off, washed with water and dried. In the X-ray diagram, no α-UO_3 lines could be observed. Upon adding NH_4OH to the filtrate, a yellow precipitate of sodium uranate was formed. The treated product, which had a specific surface area of 11 $m^2.g^{-1}$, showed a higher maximum selectivity in the reaction with toluene than the original one; however, it was still inferior to the bismuth uranate with Bi/U=2.

The influence of the calcination time and temperature on the activity was studied on a sample with Bi/U=2. Table 2-3 gives the specific surface areas, the maximum selectivities and corresponding conversions, determined under the same experimental conditions as of figure 2-3.

It appears that the best results can be obtained with a bismuth uranate with as high a surface area as possible. On the other hand, the uranates calcined under the least severe conditions will show a decay in activity during the reaction. In practice, a compromise must be made.

Table 2-3. INFLUENCE OF CALCINATION TIME AND TEMPERATURE

Calcination time (min)	Temp. (°C)	Specific Surface Area ($m^2.g^{-1}$)	Maximum Selectivity (%)	Corresponding Conversion (%)
15	500	31.6	72	79
30	500	28.0	72	83
60	500	27.0	70	84
120	500	21.4	69	79
30	600	16.2	66	80
60	600	13.4	65	77
30	700	4.9	55	77

2.6 Properties of Bi_2UO_6

The low-temperature Bi_2UO_6 is an orange-to-brown solid, easy to grind. It is slightly hygroscopic; a sample stored in air at room temperature showed a decrease in weight of 1% at 100°. Titrations on U and U(IV) were carried out at the Reactor Centrum Nederland at Petten. Total Uranium content amounted to 32.47 wt%, while the content of U(IV) was 0.55 wt%. Assuming that all Bi is in the trivalent state, the exact formula is $Bi_{1.92}UO_{5.88}$.

The IR-spectrum is given in figure 2-4 together with those of UO_3 and U_3O_8. The similarity between the spectra could be an indication that there is a resemblence between the structures of these compounds. Bi_2UO_6 also has a characteristic ESR-spectrum, depicted in figure 2-5. The signal is asymmetrical; it could not yet be ascertained to what species the signal must be attributed.

Bi_2UO_6 is stable to heat. In an atmosphere of helium, carefully freed of oxygen by a reduced BTS-catalyst, the compound can be heated up to 900° without losing weight, which proves that the oxygen partial pressure is very low.

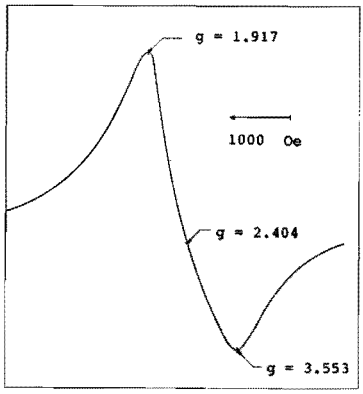

Fig. 2-5 ESR-spectrum of Bi_2UO_6

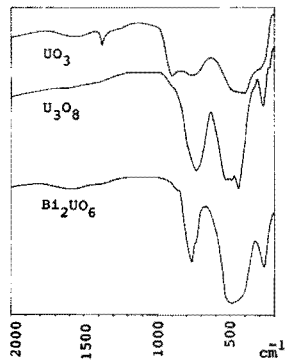

Fig. 2-4 IR spectra of UO_3, U_3O_8 and Bi_2UO_6; KBr discs

The BET-surface area of the batch (particle size 0.15-0.30 mm) that we used in our kinetic experiments was 22 $m^2.g^{-1}$. This high value indicates that the material is very porous and that the individual particles must be composed of smaller crystallites. If we assume that the skeletal density of the solid is 9 $g.cm^{-3}$ (3) and that the crystallites have the form of spheres, uniform in size, one can calculate that the crystallite radius is 135 Å. More information on this parameter, which plays an important role in the reaction kinetics, was obtained by measurements with a mercury porosimeter (Carlo Erba model). With this apparatus, the volume of mercury penetrating the porous material is determined as a function of pressure.

The pressure data are related to pore size by the following equation (10):

$$P\ r_p = 72{,}600$$

in which P is the pressure applied in atmospheres and r_p the radius of the pore that will be penetrated at the given pressure, in Å. From the experimental data the pore volume can be determined as a function of the pore size. The pore distribution curve is then derived from the former function by differentiation. Both curves are given in figure 2-6. It can be seen that the pore distribution function has a maximum at 160 Å.

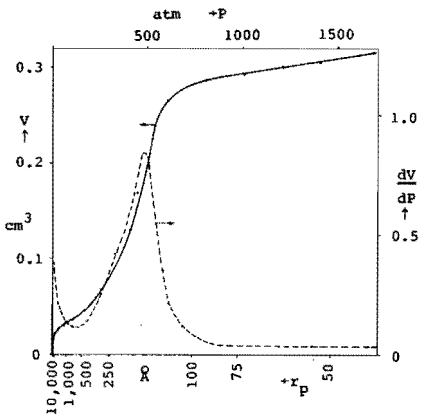

Fig. 2-6 Pore volume and pore distribution function of Bi_2UO_6 as a function of the pore radius r_p.

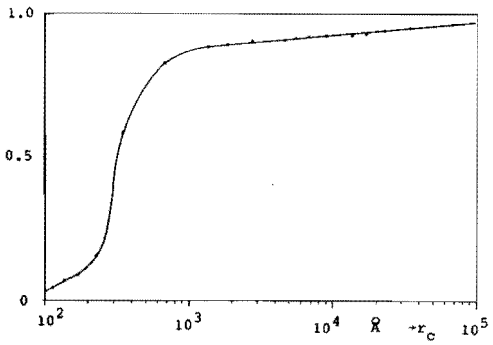

Fig. 2-7 Fraction of Bi_2UO_6 crystallites having a radius smaller than r_c as a function of r_c.

Using the approximative relation:

$$r_c = \frac{1.45 \cdot 10^5}{P}$$

a curve can be obtained representing the volume fraction of the particles having a radius smaller than r_c against r_c. Such a plot is given in figure 2-7. One finds that most crystallites have a radius of around 300 Å.

Finally, the specific surface area S can be calculated from the porosimeter data according to the equation:

$$S = 0.0016 \int_0^{V_{max}} P \, dV$$

The integral can be obtained graphically from figure 2-6. For S, a value of 36 $m^2.g^{-1}$ can now be calculated.

It will be noted that both the latter value and the crystallite radius differ from that obtained by other methods. For this effect several reasons exist: a) the soft material was crushed during the measurement in the porosimeter as a result of the high pressure applied, b) the equations used have an approximative character, and with different authors discrepancies exist between the values of the constants. c) there is considerable divergency in crystallite and pore size, the effect of which is difficult to predict.

2.7 Crystal structure of Bi_2UO_6 *

The crystal structure of Bi_2UO_6 has been briefly investigated by Erfurth (3). He proposes a hexagonal structure, a = 7.92[6], c = 19.53[2], which is a superstructure of a hexagonal cell with a = 3.96[3], c = 9.76[6], and can be visualized as a fluorite type cell with a = 5.62. Our d-values, listed in table 2-4, were computer-indexed resulting in an orthorhombic cell, a = 4.007, b = 9.689 and c = 6.875, from which a hexagonal one with a = 3.97 and c = 9.69, or a cubic one with a = 5.60 can be derived. From Guinier photographs at elevated temperatures it was seen that the orthorhombic cell is transformed into a cubic one at 1000°C. This indicates that at room temperature Bi_2UO_6 has a distorted cubic structure; from intensity measurements, however, we found that this cubic structure cannot be of the fluorite type. Work on the correct structure is still under way.

* In cooperation with Dr. A. S. Koster.

Table 2-4 d-VALUES AND INTENSITIES OF Bi_2UO_6

d	I_{obs}	d	I_{obs}	d	I_{obs}
9.731	1	1.986	37	1.525	½
4.849	8	1.952	½	1.517	½
3.467	1	1.934	4	1.463	6
3.262	100	1.851	1	1.409	6
3.244	48	1.841	2	1.399	4
3.230	44	1.717	½	1.392	5
2.823	40	1.704	20	1.387	5
2.802	21	1.692	29	1.301	6
2.426	1	1.630	11	1.291	11
2.361	3	1.620	6	1.286	8
2.030	2	1.615	5	1.266	5
2.004	13	1.542	½	1.256	7
1.993	28	1.537	½		

REFERENCES

1. Fischel, V., *Thesis*, Bern 1889, quoted in *Gmelin* 55.
2. Berman, R., *The American Mineralogist* 42, 905 (1957).
3. Erfurth, H., *Thesis*, Tübingen 1966; Rüdorff, W., and Erfurth, H., *Z.Naturforschg.* 21b, 85 (1966); Rüdorff, W., Erfurth, H., and Kemmler-Sack, S., *Z.Anorg.Allg. Chemie* 354, 281 (1967).
4. Hund, F., *Z.Anorg.Allg.Chemie* 333, 248 (1964).
5. Batist, Ph.A., Bouwens, J.F.H., and Schuit, G.C.A., *J. Catal.* 25, 1 (1972).
6. Gattow, G., and Schott, D., *Z.Anorg.Allg.Chemie* 324, 31 (1963).
7. Cordfunke, E.H.P., *J.Inorg.Nucl.Chem.* 24, 303 (1962).
8. Loopstra, B.O., and Cordfunke, E.H.P., *Rec.Trav.Chim.* 85, 135 (1966).
9. Forward, F.A., and Halpern, J., *Can.Mining and Metallurgical Bull.* oct.1953, 634.
10. Orr Jr, C., *Powder Technol.* 3, 117 (1970).

CHAPTER 3

APPARATUS

3.1 Introduction

The reaction between toluene and bismuth uranate is a gas-solid reaction. Both the products formed from the hydrocarbon and the solid oxidant have to be considered. For this purpose, three different techniques are used.

First of all, the reaction is carried out in a small tubular reactor under pulse and under continuous flow conditions. The gaseous products are analysed by gas chromatography.

In the pulse system this analysis accounts for benzene and toluene only; the remainder of the carbon is assumed to be converted into CO_2. This method is very well suited to study the reaction occurring in the stage where the oxidant is not or only slightly reduced. For measurements at a greater degree of reduction the pulse technique is not very suitable. Furthermore, results from this type of experiment often differ from those obtained under continuous flow conditions.

The flow apparatus is equipped with an on-line gas chromatographic analysis system, enabling to determine all components of the product gas. However, since the analysis time is of the order of fifteen minutes, the system is unsuitable for the examination of those stages of the reaction in which rapid changes in the reaction rates occur. Another disadvantage of the system is its low sensitivity, requiring a reasonable conversion .

Both these systems give information on the products formed from the hydrocarbon. From oxygen mass balances the degree of reduction of the oxidant can be found. The oxygen depletion can also be measured directly. For this purpose a thermobalance is

used, recording the loss of weight of a bismuth uranate sample during reduction by toluene. These measurements are very accurate, even at low reaction rates, and also prove to be very suited to determine the maximum degree of reduction.

Summarizing, the pulse , flow and thermobalance techniques each have their own merits, and the results supplement and support each other. In all three types of experiments, a fixed bed of oxidant is used, implying that there is a gradient in the toluene concentration over the bed. This, in turn, can lead to a gradient in degree of reduction of the bismuth uranate, making evaluation of the kinetic data very difficult. For that reason, most of our experiments were carried out at low degrees of conversion.

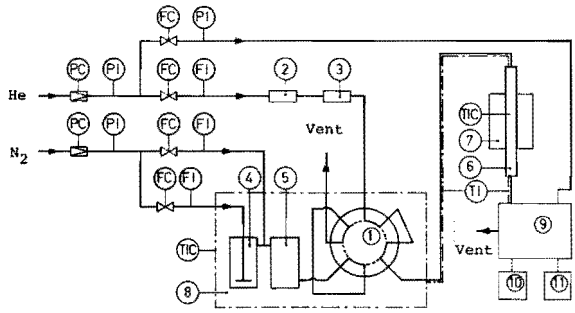

Fig. 3-1 Pulse reactor system.

1. 8-way valve
2. Tube filled with BTS-catalyst
3. Tube filled with Mol sieve
4. Vaporizer
5. Mixing vessel
6. Reactor tube
7. Furnace
8. Water bath
9. Gas chromatograph
10. Recorder
11. Electronic integrator

3.2 The pulse system

In the pulse system, depicted in figure 3-1, a constant flow of carrier gas passes through the reactor into a gas chromatograph. Pulses of a nitrogen/toluene mixture are injected before the reactor and subsequently analysed.

As carrier gas we use helium, carefully freed from oxygen by passing it over a reduced BTS-catalyst. Helium pressure in the reactor is 2.0 atmospheres absolute. Gas flow amounts to 25 $cm^3 . min^{-1}$.

Toluene/nitrogen mixtures are prepared in a vaporizer placed in a water bath. The desired nitrogen/toluene ratios can be established by varying the temperature of this bath and the primary and secondary nitrogen flows. The temperature of the bath is kept constant $\pm$ 0.2° C. From the diameter and the residence time of the nitrogen bubbles in the liquid toluene it follows that the gas leaving the vaporizer is completely in equilibrium with the liquid.

The reactor consists of a quartz tube, internal diameter 7.5 mm, heated by an electrical furnace. The bismuth uranate, usually 0.1 to 1.0 g with a particle size of 0.15-0.30 mm, is placed between two plugs of quartz wool. In experiments with 0.1 g of oxidant, a bed of quartz grains with the same particle size is used as support to obtain a fixed bed with the same height as that with 1.0 g. The temperature is measured by a stainless steel thermocouple in the middle of the fixed bed, and controlled $\pm$ 1°C with an Eurotherm Thyristor controller.

3.2.1 Analysis

Products are analysed by a Pye series 104 gaschromatograph with flame ionisation detector. We use a column, 0.5 m in length, filled with Porapak Q and kept at 185°. Benzene and toluene peak areas are determined with a Kent electronic integrator. No other products are detected. Peak areas are proportional to the concentrations in the pulse, hence:

$$(\text{toluene})_t = \frac{(A_T)_t}{(A_T)_0} \; (\text{toluene})_0$$

in which $(\text{toluene})_0$ and $(\text{toluene})_t$ denote the concentration of toluene in the pulse before and after reaction, respectively. $(A_T)_t$ is the area of the toluene peak after reaction; $(A_T)_0$ represents the toluene peak area if no reaction takes place;

it is measured before and after each experiment by replacing the oxidant-filled reactor tube with an empty one and pulsing at least four times. The areas of the "blank" peaks varied no more than 2%.

Since the sensitivity of the detector for benzene is equal to that for toluene, it follows that:

$$(\text{benzene})_t = \frac{(A_B)_t}{(A_T)_0} (\text{toluene})_0$$

in which $(A_B)_t$ represents the benzene peak area.

From these data the reaction rates can be derived. The rate of oxygen depletion of the bismuth uranate can be calculated assuming that all toluene not converted into benzene is oxidized completely to carbon dioxide and water. The results of the flow experiments, in which a complete analysis of all reaction products is made, justify this assumption.

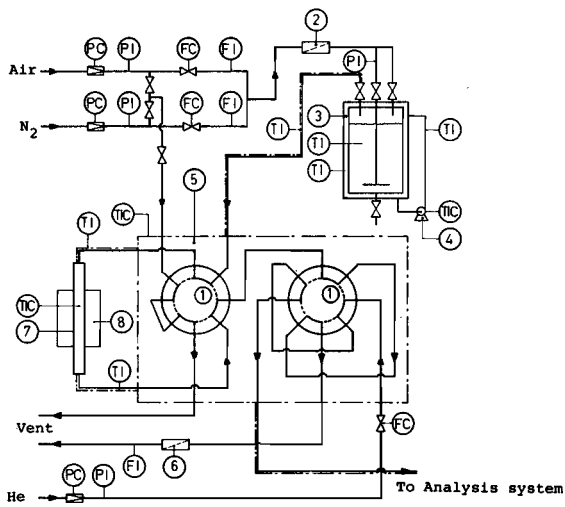

Fig. 3-2 Flow reactor system

1. 8-way valve
2. Tube filled with Mol Sieve
3. Vaporizer with water jacket
4. Circulation pump
5. Oil bath
6. Condenser
7. Reactor tube
8. Furnace

3.3 The flow system

The flow system is shown in figure 3-2. Toluene/nitrogen mixtures are prepared in a vaporizer similar to that of the pulse system. No secondary nitrogen is added. The reactor is also identical with the reactor of the pulse apparatus. Pressure in the reactor is atmospheric; pressure drop over the fixed bed is negligible.

The reactor can be by-passed by switching an 8-way valve. This allows of feeding reactant gas directly to the sampling valve and analyse it subsequently. Meanwhile, air can pass through the reactor to reactivate the oxidant. Between these reduction/reoxidation cycles, the reactor is flushed with nitrogen.

The temperature in the reactor is measured and controlled with a Eurotherm thyristor controller. During the reduction cycle, the temperature rises 2^{o} at most. But in the reoxidation step, which is more exothermic , the air has to be supplied very slowly to avoid the temperature rising above the calcination temperature of the oxidant.

From the reactor, the gases pass through a second 8-way valve which acts as a gas sampling valve for the analysis system.Volume of the sample loops is 0.500 cm^3. Pressure is atmospheric. To prevent condensation of high boiling products, all pipes are heated electrically while the two 8-way valves are immersed in a silicon-oil bath kept at 100^{o}.

3.3.1 Analysis

In the flow apparatus a quantitative analysis of all components of the reaction mixture was required. These components are: benzene, toluene, CO, CO_2, H_2O, N_2 and biphenyl. We chose for a gaschromatographic analysis, mainly because of the short analysis time and the simplicity and accuracy of this method, and decided to neglect the small amounts of biphenyl formed.

The system is represented in figure 3-3. It consists of four GLC columns, three of which are connected in series, and

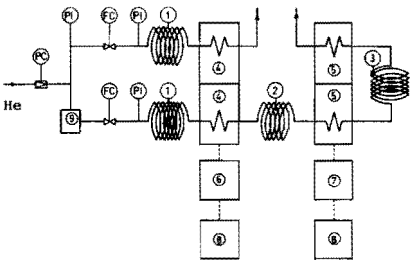

1. Column Porapak Q, 185°C
2. Column Porapak Q, 48°C
3. Column Mol Sieve 13X, 25°C
4. Pye thermal conductivity detector
5. Becker thermal conductivity.detector
6. Pye amplifier
7. Becker amplifier
8. W&W recorder with integrator
9. Gas sampling valve

Fig. 3-3 Analysis system

two double thermal conductivity detectors. On the first column (0.5 m, Porapak Q, 185°) the product gas is separated into benzene, toluene and a mixture of CO, CO_2, H_2O, N_2 and O_2. The components pass a thermal conductivity detector which records three peaks: one of benzene, one of toluene and one of the other gases. A second, identical column is switched parallel to the first, allowing of the application of temperature programming. This can be of advantage should higher boiling components have to be determined. The effluents from the first column pass to a second one (2.0 m, Porapak Q, 48°). Here, the products are separated into CO_2, H_2O and a mixture of CO, N_2 and O_2; benzene and toluene remain on the column and are removed occasionally by heating the column to 150°. Three peaks are detected: one for the permanent gases, one for CO_2 and one for H_2O. Finally, the permanent gases are separated on a third column (4.0 m, Molsieve 13X, room temperature) where CO, N_2 and O_2 can be determined. CO_2 and H_2O are retained by the column; a frequent regeneration at 200° is therefore required.

Since the last two detectors are connected to one amplifier and recorder, it is necessary to choose the lengths and the temperatures in such a way that never two peaks are recorded at the same time. One of the detectors has always to serve as a reference for the other. As a result, the polarity of the

peaks of CO_2 and H_2O is opposite to that of the peaks of O_2, N_2 and CO. Peak areas are determined with W&W recorders equipped with electronic integrators. The chromatograms of a typical sample of product gas, in which CO and O_2 were absent, are shown in figure 3-4.

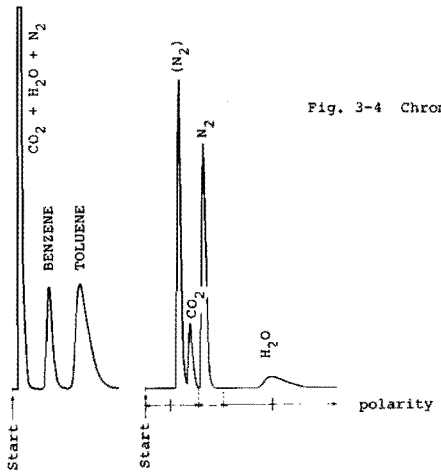

Fig. 3-4 Chromatograms of the oxidation products of toluene

Pressure build-up over the three columns in series is considerable. With a carrier gas pressure of 5 atmospheres, gas flow is 40 $cm^3 . sec.^{-1}$. Total analysis time is 15 minutes. If, as in some experiments, only benzene and toluene have to be determined, an analysis will take 5 minutes.

To determine the various components of the reaction mixture quantitatively, an internal standard should be added. Since nitrogen does not participate in the reaction between toluene and bismuth uranate it can serve as such. If we assume that the peak area of a component is proportional to its mole fraction, the following relation can be derived:

$$\frac{X_x}{X_{N_2}} = \frac{\phi_x}{\phi_{N_2}} = f_x \cdot \frac{A_x}{A_{N_2}}$$

X_x: mole fraction of component x
X_{N_2}: mole fraction of nitrogen

ϕ_x: mole flux of component x
ϕ_{N_2}: mole flux of nitrogen
f_x: response factor of component x
A_x: peak area of component x
A_{N_2}: peak area of nitrogen

The response factor f_x can be determined experimentally according to two different methods.

In the first method, mixtures of known composition are analysed. f_x can be calculated with the equation given above. Mixtures of nitrogen and benzene, toluene or water are prepared in the vaporizer. The mole fractions of these compounds follow from the vapour pressures. Mixtures of nitrogen and oxygen, CO or CO_2 are obtained with two Wösthoff plunger pumps.

In the other method, a sample of a mixture of a compound x and nitrogen is analysed, followed by a sample of pure nitrogen, both at the same pressure and temperature . The peak area of the pure nitrogen sample will be called $A_{N_2,O}$.
As:

$$X_{N_2} = \frac{A_{N_2}}{A_{N_2,O}}$$

and:

$$\sum f_{x_i} A_{x_i} = \sum \frac{A_{N_2} X_{x_i}}{X_{N_2}} = \frac{A_{N_2}}{X_{N_2}} \sum X_{x_i} = A_{N_2,O}$$

it follows that if we analyse a mixture of N_2 and a component x:

$$f_x A_x + A_{N_2} = A_{N_2,O} \quad \text{and:} \quad f_x = \frac{A_{N_2,O} - A_{N_2}}{A_x}$$

Since all variables in the right hand side of this equation are known, f_x can be calculated.

It is clear that with this method the concentration of the component x in the sample may remain unknown. This could be advantageous should we want to determine the response factor of a compound of which no vapour pressure data are known. We also can check, by comparing the values for f_x obtained by these two methods, whether the mole fraction of the component x in the gas leaving the vaporizer is in agreement with the value calculated from the vapour pressure. In this way we were able to ascertain that the saturation in the vaporizer was complete indeed.

During the experiments $\sum f_{x_i} A_{x_i}$ was calculated for each analysis. If the value deviated from $A_{N_2,0}$, the analysis results were considered unreliable and put aside. From the analytical results atom balances are calculated. Usually about 98% of the C and H atoms fed to the reactor can be accounted for.

Before the reaction the bismuth uranate bed is purged with nitrogen. When the reaction is started, the feed gas mixes up with this nitrogen and the actual hydrocarbon concentration is lowered. This leads to an apparent deficiency in C and H in the analysis results during the very first stages of the reaction. It also prohibits the accurate establishment of the time at which the process is started.

3.4 Thermobalance

The thermobalance apparatus is shown in figure 3-5. The instrument used is a Dupont 900/950 thermal analyser. The sample chamber consists of a quartz tube, i.d. 4 cm, heated by an electric furnace. The sample is placed in a platinum boat, attached to one arm of a microbalance. The sample chamber is at atmospheric pressure and can be flushed with a toluene/nitrogen mixture prepared as usual. The nitrogen used was made oxygen-free by passing it over a reduced BTS-catalyst, and dried. The temperature in the sample chamber is measured with a thermocouple placed just above the sample holder. Operations are carried out under isothermal conditions. Experiments with the thermocouple in the middle of the oxidant

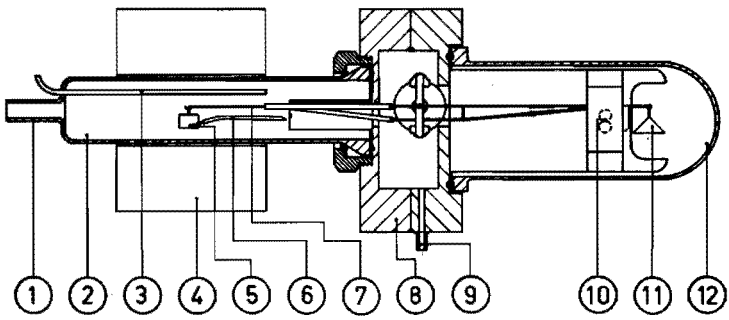

Fig. 3-5 Thermobalance apparatus

1. Feed gas inlet
2. Quartz furnace tube
3. Gas outlet
4. Furnace
5. Sample boat
6. Thermocouple
7. Quartz tube
8. Balance housing
9. Purge gas inlet
10. Photo-voltaic cells
11. Counter-weight pan
12. Pyrex envelope

bed showed that the rise in temperature during the reaction is 2^{o} at most.

The sample, usually around 20 mg, is placed on a flat platinum foil of 5 x 10 mm. This means that the thickness of the layer of solid is of the order of a few particle diameters, ensuring a good heat transfer and a good accessibility of the toluene to the sample.

To avoid the presence of toluene vapour in the other side of the balance, where the weight changes are recorded with photoelectric cells, this part of the system is purged with nitrogen. Both gas flows leave the balance through a small tube ending under water to prevent back diffusion of oxygen.

The sensitivity of the thermobalance is 0.01 mg. This corresponds to an error in the degree of reduction of the bismuth uranate of 0.4%.

CHAPTER 4

THE REACTION BETWEEN TOLUENE AND BISMUTH URANATE

4.1 Introduction

The peculiar oxidation properties of bismuth uranate were first discovered during a study on the air oxidation of toluene to benzaldehyde over various oxide catalysts *. It was found, rather surprisingly, that, using an air/toluene ratio of 0.2 and a reaction temperature between 400 and 500°C, considerable amounts of benzene were produced over a bismuth uranate catalyst. However, the activity of this catalyst sharply declined with time. By passing air over the solid the original activity was restored. By carrying out the reaction in a glass microreactor, heated by a movable furnace, we were able to observe the catalyst during the process. It was seen that bismuth uranate, originally orange, turned green and, finally, black, beginning from the exit of the catalyst bed. Only where the feed gases entered the reactor did it keep its original colour. The benzene production was maximum when the largest part of the catalyst was green. Upon reactivation with air the yellow colour reappeared.

Since the same colour changes occurred when bismuth uranate was partially reduced by hydrogen, we concluded that the different colours correspond to different stages of reduction. Apparently, bismuth uranate is reduced during the reaction with toluene, except for the place where the feed gas enters the reactor and the oxygen pressure is high. It became also clear that benzene is produced mainly on the partially reduced catalyst. Therefore, attempts were made at various air/toluene ratios, temperatures and contact times to carry out the reaction continuously with a green catalyst. Unfortunaly, all these attempts were unsuccessful. When the air/toluene ratio was

* These investigations will be dealt with in chapter 7.

increased, the yellow layer broadened and the benzene production went down. In the extreme case that so much oxygen was added that the whole bed was yellow, no benzene was formed at all, and most of the toluene underwent total combustion.

Experiments were also carried out when no air was present, using a toluene/nitrogen mixture as the feed gas. The catalyst now actually acted as an oxidant. It was seen that in the initial stages, i.e. with a fully oxidized catalyst, almost all toluene was converted into CO_2 and H_2O. After a few per cent of the oxygen of bismuth uranate had been used up, benzene production rapidly increased, reached a maximum and finally declined. After such a run, the bismuth uranate was black. When exposed to air at room temperature, a vehement and exothermic reaction took place. Temperature rose to 400-500^{o} and the yellow colour reappeared. We can now understand why this catalyst shows such an extraordinary behaviour. If oxygen and toluene are fed over a fully oxidized catalyst, the toluene is completely combusted. This reaction proceeds until all oxygen is consumed. Thereafter, the excess toluene is oxidized by the lattice oxygen of the bismuth uranate. The latter substance is reduced and eventually loses its activity.

Starting with a partly reduced catalyst, it should theoretically be possible to achieve a steady state and to produce benzene continuously from toluene and air. However, the oxidation of the reduced bismuth uranate by molecular oxygen proceeds so much faster than its reduction by toluene that the bismuth uranate will immediately regain its fully oxidized, hence unselective, state. Evidently, to achieve a high benzene production, the reaction must be carried out in two separate steps:

$$xC_7H_8 + Bi_2UO_6 \rightarrow xC_6H_6 + xCO_2 + xH_2O + Bi_2UO_{6-3x}$$

$$Bi_2UO_{6-3x} + 3x/2\ O_2 \rightarrow Bi_2UO_6$$

This can be materialized by passing air and a toluene/nitrogen mixture over a fixed bed of bismuth uranate alternately. In this way approximately 50 grams of toluene can be converted into benzene with 1 kg of bismuth uranate, the overall selectivity being of the order of 2/3. The process can be repeated as often as required. We have performed up to 50 cycles with the same batch of bismuth uranate without observing any decrease in activity.

The demethylation process described so far, is applicable for the dealkylation of other alkylaromatics as well. Experiments carried out by Heynen (1) showed that a blend of several alkylbenzenes, b.p. 161-181°, commercially available as "Shellsol A", could be almost completely converted into benzene by passing it over bismuth uranate. He also found that methylnaphtalene can be demethylated to naphtalene in the same way. However, in the following we confine ourselves to the demethylation of toluene.

4.2 Reaction products from toluene

The products formed from toluene were determined gaschromatographically in the continuous flow system described in chapter 3. Benzene, carbon dioxide and water accounted for about 98% of the C and H atoms of the toluene converted. The reaction products, condensed in a trap cooled with a dry ice/acetone mixture were subjected to GLC analysis (column: polyphenylether, length 2 m). Traces of benzaldehyde were detected. Sometimes a white solid deposited in the colder parts of the flow reactor system. Odour, IR and PMR spectra of this material were characteristic of diphenyl. In the pulsereactor system, already described in chapter 3, small amounts of methane and ethane were found, expecially if the reaction temperature was high and the degree of reduction of the bismuth uranate was low.

4.3 Reaction products formed from Bi_2UO_6

If one wants to examine the solid phases formed by reduction of Bi_2UO_6, special care has to be taken to prevent reoxidation of the material. For that reason we built a flow reactor system,

identical with that described in chapter 3 but without the analysis system, and placed it inside a glove box, purged with nitrogen. In this apparatus samples of Bi_2UO_6 were reduced in the usual way. At given time intervals the reactor was opened and a small aliquot of the solid was transferred to a Lindemann glass capillary which was sealed immediately within the glove box and thereafter could be handled in the atmosphere.

Experiments were carried out with two batches of bismuth uranate, the first of which was calcined during 1 hour at 700°C, and the second during 1 hour at 500°. As has already been shown in chapter 2, the diffraction lines of the former sample are well defined, allowing of an accurate determination of the cell parameters. With the latter, the lines are more diffuse, but it was with this sample that most of the kinetic runs in the pulse system and the thermobalance were performed. Both samples were reduced under the following conditions: toluene mole fraction 0.003, temperature 470°. From experiments carried out under the same conditions in the thermobalance the degree of reduction was determined as a function of time. This provided us with a degree of reduction α of the samples in the capillaries. These were 10, 16 and 27%, respectively, for the 500°-sample, and 4, 7, 10, 13, 15 and 17%, respectively, for the 700°-calcined bismuth uranate. The X-ray diffraction data of the samples were obtained with a Debye-Scherrer camera, using Ni-filtered Cu radiation. It appeared that the only phases detectable were metallic Bi and Bi_2UO_6. The changes in the d-values of Bi_2UO_6 with increasing α where within the experimental error. Bismuth metal was present in all samples, even in that having a degree of reduction of a mere 4%. The intensities of the bismuth lines increased with α. Similar results were obtained from samples reduced under pulse conditions.

To get an impression of the crystallite size of the bismuth metal particles, Debye-Scherrer photographs were made, both with and without rotation of the sample capillary. Without rotation, dark spots were visible amidst the bismuth lines; they were invisible when the tube was rotated. This indicates, that some of the particles have a diameter between 10 and 50 μ. In the lines of bismuth uranate no spots were to be seen. The presence of such large bismuth crystallites proves that the bismuth atoms have a tendency to fuse to larger conglomerates as soon as they are

formed. This is not surprising since bismuth is liquid at the reaction temperature (m.p. 273°C). It is also in agreement with the work of Bradhurst and Buchanan (2) who studied the properties of liquid bismuth on oxide surfaces, in particular on UO_2. They found complete absence of wetting of the solid surface by the liquid metal. This means that, if a thin layer of metallic Bi is formed on an oxidic surface, it will readily form drops with as little contact area with the oxide as possible. Upon cooling, these drops form the larger crystallites visible in the X-ray diagrams.

When metallic bismuth is formed and removed out of the Bi_2UO_6 lattice, a uranium-rich phase must remain. No uranium oxide phase was detectable. In the second chapter of this thesis we observed that even small amounts of excess α-UO_3 in Bi_2UO_6 could be seen in the X-ray diagrams. Apparently, α-UO_3 is absent in the reduced bismuth uranate. But then, the presence of α-UO_3 was not expected, since we know that UO_3 is rapidly reduced by toluene to form UO_2. Most probably the uranium-rich phase consists of finely dispersed UO_2 in Bi_2UO_6. The amounts of UO_2 dissolved are small. At α=25%, the UO_2 content of the solid phase does not exceed 18% by wt.

We also carried out an experiment in which Bi_2UO_6, calcined for 1 hour at 500°, was reduced with hydrogen at 850° for several hours. In this sample, bismuth metal and a cubic phase were present. Evidently, a complete collapse of the Bi_2UO_6 structure to the cubic UO_2 structure had occurred.

4.4 A qualitative reaction model

With the above results, we can visualize the reduction of Bi_2UO_6 by toluene as follows: toluene reacts at the surface of the solid under the formation of benzene, CO_2 and H_2O. Oxygen atoms are removed from the surface and replenished by diffusion from the bulk. Bi^{3+} and U^{6+} ions are reduced to Bi-metal and U^{4+}, respectively. The zerovalent Bi atoms leave their original positions to form spheres of molten Bi, some of which are even larger than the original Bi_2UO_6 crystallites. Thus the bismuth and oxygen ions are progressively removed out of the bismuth uranate structure, which eventually collapses to form a UO_2 structure. Attention is drawn to the fact that not all oxygen

atoms can be removed, but that the reaction ends at the composition Bi_2UO_2. This will also be demonstrated thermodynamically in section 5 of the present chapter.

Upon reoxidation the reverse reactions take place. The metallic bismuth is oxidized to Bi_2O_3 which reacts with the uranium-rich phase to form Bi_2UO_6. The latter reaction is similar to the one occurring during the preparation and calcination of our low-temperature Bi_2UO_6 described in chapter 2. The rate of this reaction depends on the crystallite size of the participating oxides. The size of the bismuth oxide particles depends, in turn, on the dimensions of the bismuth metal clusters and hence on the conditions during the reduction, high reduction temperatures and long reduction times favouring the formation of large bismuth conglomerates. This is in agreement with the observation that the more a sample is reduced, the more difficult becomes its complete reoxidation. It was observed that with the hydrogen-reduced sample this reoxidation process is very slow. This can also explain the rather poor reproducibility of experiments in the flow reactor system. Should in any of these experiments a large bismuth metal particle have formed, the subsequent reoxidation cycle might have been insufficient for a complete restoration of the Bi_2UO_6 structure, leading to the presence of free bismuth and uranium oxides in the oxidant.

It is interesting to compare these results with the work of Swift, Bozik, Ondrey, Massoth and Scarpiello (3, 4) on the oxidative dimerisation of propylene using bismuth oxide as oxidant. In this process a N_2/propylene mixture is passed over Bi_2O_3 at 520^{o}. The bismuth oxide is reduced to metallic Bi, but can be reoxidized afterwards, provided that the reduction is not carried too far. Samples of unsupported Bi_2O_3 from which up to 60% of the oxygen atoms had been removed could be rapidly regenerated to the original activity by heating in air at the reaction temperature. Samples reduced beyond 60% could, even after a 16-hour heat treatment with air, not be reoxidized completely, lines of Bi-metal remaining observable in the X-ray diagrams. Apparently the bismuth metal crystallites had become too large to be reoxidized within 16 hours. On the other hand,

alumina - supported bismuth oxide could be reduced to the metallic state and reoxidized without any decay of activity. Here, the bismuth particles remain dispersed within the pores of the support, preventing coalescence to large particles. This suggests that the problem of clustering of bismuth metal particles which are difficult to reoxidize, encountered during the reduction of bismuth uranate, can be solved by using a supported bismuth uranate.

There are many parallelisms between the compounds Bi_2UO_6 and Bi_2MoO_6. Bismuth molybdate is capable of demethylating toluene to a small extent (see chapter 7) and it can be reduced by hydrocarbons and reoxidized. Eventually reduction with butene results in the formation of Bi metal and MoO_2. For that reason it does not seem irrealistic to assume that already in the initial stages of the reduction of Bi_2MoO_6 metallic bismuth forms, in the same way as with Bi_2UO_6.

In a recent paper, Matsuura and Schuit (5) remarked that bismuth molybdate samples reduced at low temperatures were reoxidized more rapidly than others which were reduced at higher temperatures or reduced at low temperatures but subsequently heated to high temperatures. It appeared that not the conditions during reduction but only the temperature to which the reduced samples were exposed and the heating time were responsible for these differences. The authors attributed this effect to a rearrangement of the bulk structure of Bi_2MoO_6 during the heat treatment. We now feel that this rearrangement might consist in the formation of large bismuth metal crystallites. The lower the temperature and the shorter the time of heating, the less the tendency of bismuth metal to form larger conglomerates, hence the more rapid the reoxidation step will proceed.

Other indications of the formation of metallic bismuth during the reduction of Bi_2MoO_6 were obtained in our laboratory by Lankhuijzen (6). He studied the ammoxidation of propylene over this catalyst and found that once the oxygen to hydrocarbon ratio in the feed gas had been too low, the selectivity for acrylonitrile decreases due to extensive ammonia combustion. This can be explained by assuming that during the period of oxygen shortage in the feed, the catalyst is reduced under the formation

of metallic Bi particles. If these are reoxidized to Bi_2O_3 later on, the ammonia will be converted into N_2 and H_2O on the bismuth oxide surface, since Bi_2O_3 is an effective catalyst for the NH_3 combustion.

4.5 Thermodynamics

In the preceding sections it was described that the end product obtained by reduction of Bi_2UO_6 was composed of a mixture of metallic bismuth and UO_2. It is interesting to calculate whether this is also the thermodynamic equilibrium composition. This should be possible provided that the thermodynamic constants are available. This is, however, not the case. Therefore,we first calculated ΔG and ΔH for the reaction between toluene and the oxides of bismuth and uranium separately; thereafter we made some assumptions to find approximative values for ΔG and ΔH for the reaction between toluene and Bi_2UO_6. To start with, ΔG_f and ΔH_f were calculated for each of the components at 750 K (477°C), taking the elements at 25°C and 1 atmosphere as standard state. The results are given in table 4-1.

TABLE 4-1 HEAT OF FORMATION AND FREE ENERGY OF FORMATION OF A NUMBER OF SUBSTANCES AT 1 ATMOSPHERE AND 750 K, IN KCAL.MOLE^{-1}, TAKING THE ELEMENTS AT 25°C AS STANDARD.

	ΔG_f^{750}	ΔH_f^{750}	Reference
Bi_2O_3	-172	-125	7
Bi (l)	- 13	+ 6	7
α-UO_3	-325	-292	7
U_3O_8	-962	-869	7
UO_2	-288	-262	7
α-U	- 11	+ 4	7
C_7H_8	- 53	+ 30	8
C_6H_6	- 35	+ 35	8
CO_2	-135	- 89	7
H_2O	- 97	- 48	7
O_2	- 38	+ 3	7

Next we listed a number of possible reactions and calculated ΔG_r^{750} and ΔH_r^{750}:

		ΔG_r^{750}	ΔH_r^{750}
$Bi_2O_3 + 1/6C_7H_8$	$\rightarrow 2Bi + 7/6CO_2 + 2/3H_2O$	-67	-4 KCAL.MOLE^{-1}
$Bi_2O_3 + C_7H_8$	$\rightarrow 2Bi + C_6H_6 + CO_2 + H_2O$	-66	+3
$UO_3 + 1/54C_7H_8$	$\rightarrow 1/3U_3O_8 + 7/54CO_2 + 2/27H_2O$	-19	-13
$UO_3 + 1/9C_7H_8$	$\rightarrow 1/3U_3O_8 + 1/9C_6H_6 + 1/9CO_2 + 1/9H_2O$	-20	-12
$1/3U_3O_8 + 1/27C_7H_8$	$\rightarrow UO_2 + 7/27CO_2 + 4/27H_2O$	-15	-4
$1/3U_3O_8 + 2/9C_7H_8$	$\rightarrow UO_2 + 2/9C_6H_6 + 2/9CO_2 + 2/9H_2O$	-15	-2
$UO_2 + 1/9C_7H_8$	$\rightarrow U + 7/9CO_2 + 4/9H_2O$	+135	+172
$UO_2 + 2/3C_7H_8$	$\rightarrow U + 2/3C_6H_6 + 2/3CO_2 + 2/3H_2O$	+134	+178
$UO_2 + 1/3O_2$	$\rightarrow 1/3U_3O_8$	-20	-29
$1/3U_3O_8 + 1/6O_2$	$\rightarrow UO_3$	+2	-3
$2Bi + 3/2O_2$	$\rightarrow Bi_2O_3$	-89	-142

It can be seen that bismuth oxide is easily reduced to the metal, and that the caloric effect of this reaction is comparatively slight. Uranium oxide can be reduced to uranium dioxide, but not to the metal.Upon reoxidation with molecular oxygen Bi_2O_3 and U_3O_8 will be formed; these reactions are exothermic. To find ΔG_r^{750} and ΔH_r^{750} for the overall reaction between Bi_2UO_6 and toluene, the thermodynamic constants of the reaction: $Bi_2O_3 + UO_3 \rightarrow Bi_2UO_6$ should be known. These constants are not available. Assuming that $\Delta G_r^{750} = x$, and $\Delta H_r^{750} = y$, we obtain the following data:

$$Bi_2UO_6 + 2/9C_7H_8 \rightarrow 2Bi + UO_2 + 14/9CO_2 + 8/9H_2O$$

$$\Delta G_r^{750} = -x - 101 \qquad \Delta H_r^{750} = -y - 21$$

$$Bi_2UO_6 + 4/3C_7H_8 \rightarrow 2Bi + UO_2 + 4/3C_6H_6 + 4/3CO_2 + 4/3H_2O$$

$$\Delta G_r^{750} = -x - 102 \qquad \Delta H_r^{750} = -y - 9$$

$$2Bi + UO_2 + 2O_2 \rightarrow Bi_2UO_6$$

$$\Delta G_r^{750} = x - 107 \qquad \Delta H_r^{750} = y - 173$$

These results indicate that the reduction of Bi_2UO_6 to Bi and UO_2 is, thermodynamically, a favoured reaction as long as x is greater than 100 kcal.mole^{-1}. In view of literature data on comparable reactions we expect a much higher value for x. Furthermore it is evident that most of the heat of reaction is evolved during the reoxidation step.

4.6 Industrial applications

The use of a two-step discontinuous process seems to be a serious disadvantage for application on an industrial scale. However, this can be overcome if, instead of a fixed bed of bismuth uranate in contact with toluene and air intermittently, a fluidized catalyst is used, circulating between two reactors. In the first reactor, toluene is oxidized to benzene, and in the second the reduced bismuth uranate is regenerated by air (fig. 4-1).

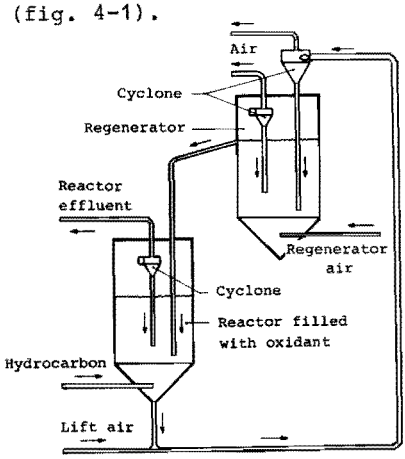

Fig. 4-1 Reactor system with two fluid beds

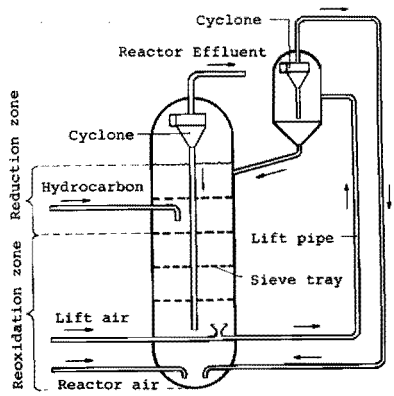

Fig. 4-2 Dual zone fluid bed reactor

Similar installations, containing up to 400 tons of catalyst, are used in the petroleum industry for the process of catalytic cracking. Here, the regeneration of the catalyst is required because of the coke-formation on the catalyst surface. In these systems, the weight ratio of catalyst to hydrocarbon is of the order of 10, while for the demethylation process a value of 20 was calculated. On the other hand, the demethylation is fast, allowing of low contact times and a small reactor as compared with the cracking reaction.

Solid particles to be used in a fluidized bed must be very strong, since it is impossible to recover all fine dust, formed by attrition of the heavely agitated solid. This material would be lost and also pose a considerable problem in view of air polution. Bismuth uranate itself is rather soft, hence it is necessary to use a supported material, e.g. bismuth uranate on silica.

Even more convenient than a twin fluid-bed system seems to be a single fluid-bed reactor with separate oxidation and reduction zones as described by Callahan (9). Air and hydrocarbons enter the reactor at different places while the catalyst circulates between the two zones (fig. 4-2). This system is in full commercial use for the ammoxidation of propylene. One fact, however, probably prohibits the application of the title reaction on an industrial scale, namely the vapour pressure (10^{-4} mm) of the Bi-metal (10). Assuming that the reactant gas is completely saturated with bismuth vapour, we calculated that with each reaction cycle approx. 1.5 mg of Bi per kg Bi_2UO_6 is removed. Although this material could be recovered behind the reactor, its removal from the bismuth uranate implies that the Bi/U ratio in the latter is reduced. This, in turn, will eventually cause a decrease in selectivity.

REFERENCES

1. Heynen, H.W.G., unpublished results.
2. Bradhurst, D.H., and Buchanan, A.S., *Aust.J.Chem.* 14, 409 (1961).
3. Swift, H.E., Bozik, J.E., and Ondrey, J.A., *J.Catal.* 21, 212 (1971).
4. Massoth, F.E., and Scarpiello, D.A., *J.Catal.* 21, 225 (1971).
5. Matsuura, I., and Schuit, G.C.A., *J.Catal.* 25, 314 (1972)
6. Lankhuijzen, S.P., unpublished results.
7. *Handbook of Chemistry and Physics*, The Chemical Rubber Co., 51st edition, Cleveland, 1970.
8. Landolt-Börnstein, *Zahlenwerte und Funktionen*, band IV, Springer-Verlag, Berlin, 1961.
9. Callahan, J.L., and Milberger, E.C., *U.S.P.* 3,472,892 (1969).
10. Nesmeyanov, A.N., *Vapor Pressure of the Chemical Elements*, Elsevier, Amsterdam, 1963.

CHAPTER 5

KINETICS

5.1 Pulse experiments

The conditions under which the pulse experiments were carried out are given in table 5-1.

Table 5-1 Reaction conditions during pulse experiments

Pulse interval	: 6 min
Pulse volume	: 0.534 cm^3
Gas flow	: 25 $cm^3.min^{-1}$
Reaction pressure	: 2 atm
Reaction temperature	: 430 - 515°C
Amount of Bi_2UO_6	: 0.1 - 1.0 g
Particle size	: 0.15 - 0.70 mm
Toluene mole fraction	: 0.006 - 0.09

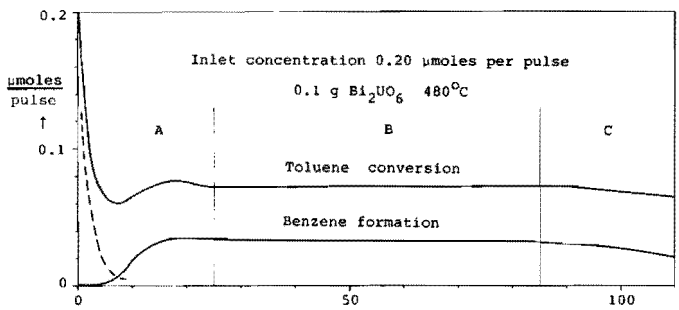

Fig. 5-1 Reaction rates as a function of the number of pulses N

First it was established that no reaction takes place in the empty reactor. When an experiment is carried out under the conditions listed above and the rate of conversion of toluene and the rate of formation of benzene are plotted against the number of pulses N, figures are obtained of which fig. 5-1 is a typical example. Although the reaction rates may vary with the batch of bismuth uranate, the curve has always the same shape. Three different regions can be clearly distinguished, to be called regions A, B, and C, respectively. In region A the

conversion rapidly decreases with increasing N and reaches a minimum, and at the same time the benzene formation rate increases. In region B both reaction rates are constant, while they decline in region C.

5.1.1. Region A

The peculiar form of the curves in region A can be accounted for by assuming that the toluene conversion is actually the sum of two different processes, a fast non-selective oxidation, declining with N, and a more selective oxidation, the rate of which increases upon reduction of the bismuth uranate.

If, instead of a toluene/nitrogen mixture, a benzene/nitrogen mixture is used as the feed gas, a curve is obtained for the benzene oxidation rate which is depicted in fig. 5-1 as a broken line. Obviously, the aromatic nucleus is rapidly attacked in region A, and is almost stable in region B. One could imagine this type of non-selective oxidation to be due to the presence of molecular oxygen, adsorbed on the fully oxidized bismuth uranate surface. However, before each experiment the bismuth uranate was heated for approximately 1 hour at the reaction temperature in a flow of oxygen-free helium, during which period O_2 would have to desorb. Even heating the oxidant in a helium flow for several hours at 550°C had no influence on the reaction rates. A sample of fresh bismuth uranate heated in vacuo at 600°, desorbed an amount of 4 μmoles of oxygen, corresponding to a degree of reduction of 0.001 *.

Another explanation for the difference in behaviour of the bismuth uranate in the regions A and B could be that initially the surface is covered with unselective sites, which are successively poisoned by adsorption of hydrocarbons during the reaction. The following objections can be made to this assumption:

1. Since the adsorbed hydrocarbons should slowly desorb in the time between the pulses, the length of the pulse interval

* Experiment carried out by Dr. I. Matsuura

should affect the reaction rates. This proved not to be the case.

2. An experiment was carried out in which we stopped pulsing at the beginning of region B, heated the oxidant at 100° above the usual reaction temperature in helium, kept it at that temperature for one hour, and then continued the run under the original conditions. During this heat treatment no hydrocarbon desorption could be observed by gas chromatography. Furthermore, the reaction rates after this heat treatment were unchanged.
3. Finally, we determined the amount of adsorbed hydrocarbon in the following way; after a given number of pulses the reactor and the gas chromatograph were disconnected, and to the former a tube containing magnesium perchlorate was attached. Behind this tube, a second one was placed, filled with a mixture of ascarite and magnesium perchlorate. Air was passed over the oxidant. Adsorbed hydrocarbons and "coke" were oxidized completely into CO_2 and H_2O, the latter of which was adsorbed in the first tube and the former in the ascarite-filled one. The amount of CO_2 and hence the quantity of adsorbed hydrocarbons followed from the difference in weight of the second tube before and after an experiment. The accuracy of this method was 0.05 mg of C.

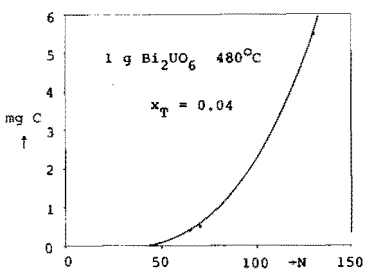

Fig. 5-2 Amount of carbon deposited as a function of the number of pulses N

In fig. 5-2 the amount of carbon is given as a function of the number of pulses N. Under the prevailing conditions region A ends at about N=10. It appears that in the initial stages of the reaction the amount of adsorbed hydrocarbon is very small; consequently it is very unlikely that the reaction rates are influenced by this adsorbate.

Furthermore it was established that during a pulse experiment the surface area of the bismuth uranate as determined by the BET-method under nitrogen, remains unchanged. Assuming that the converted toluene, not transformed into benzene, is oxidized to CO_2 and H_2O (which assumption is to a great extent justified by the results of the flow experiments to be described below), we also calculated the amount of oxygen consumed, the degree of reduction α, defined as the

number of oxygen atoms removed divided by the number of oxygen atoms present in fully oxidized bismuth uranate, and the rate of oxygen disappearance -dO/dt. Plotting the reaction rates as measured with bismuth uranates having different specific areas, against α, one obtains the picture of fig. 5-3. Evidently, with every sample region A ends at the same value of α. Although this does not necessarily mean that the degree of reduction at the surface is always equal to that of the bulk, in pulse experiments it is unlikely that a gradient in oxygen content over the oxide crystallite exists. Such a gradient would level out in the time between the pulses, as will be shown in the discussion of this chapter.

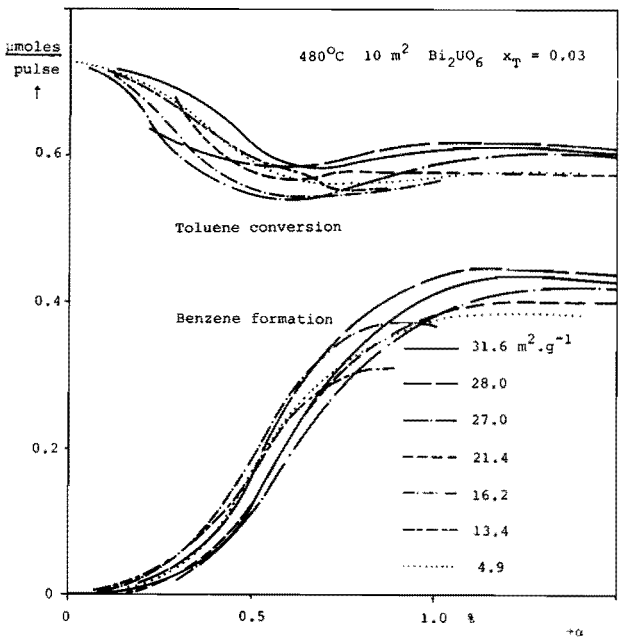

Fig. 5-3 Reaction rates as a function of the degree of reduction for different bismuth uranates

These results strongly suggest that the rapid and unselective oxidation in region A is due to the presence of a special kind of oxygen, which is present on or can be supplied from the fully oxidized bismuth uranate in a fixed percentage of the mass. The available number of these non-selective A-oxygen atoms bears little relation to the surface area of the oxidant and therefore may not be considered as the surface oxygen layer.

5.1.2. Region B

In region B the reaction rates are independent of the degree of reduction of the oxidant, in other words the reaction is zero order in oxygen. The reason why the reaction rates do not change in this region will be discussed later on in this chapter. In any case it enables the determination of the influence of the toluene concentration and the reaction temperature on the reaction rates in this region.

It was established that the rates are a function of the reaction conditions in region B only and are unaffected by the conditions under which region A is passed. We started every experimental run with fresh oxidized catalyst, and after passing region A took the average value of five pulses as the B-reaction rate.

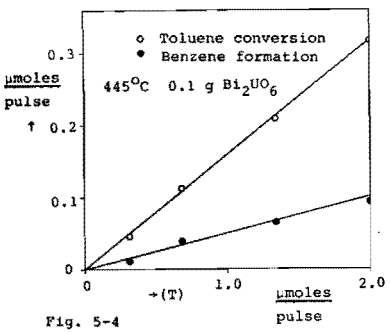

Fig. 5-4

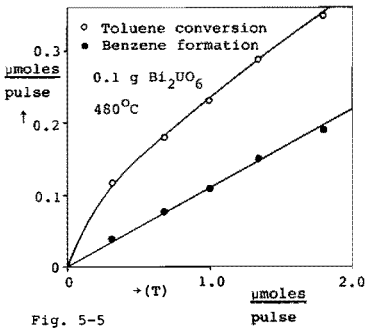

Fig. 5-5

Reaction rates as a function of the toluene inlet concentration (T); pulse system

As can be seen from fig. 5-3, the rate of toluene conversion per unit of surface area is almost uninfluenced by the specific surface area. The rate of benzene formation is a more pronounced function of the specific surface area, probably as a result of differences in surface properties of the bismuth uranate. Fig. 5-4 gives the reaction rates as a function of the toluene inlet concentration at a reaction temperature of 445°C. It appears that both the rate of toluene conversion and that of benzene formation are first order in toluene. The reaction can be described by the following model:

Toluene → Benzene + CO_2 + H_2O (selective)

Toluene → Other oxidation products (non-selective)

$$-\frac{d(T)}{dt} = k_1 (T) \qquad (1) \quad \text{and :}$$

$$\frac{d(B)}{dt} = k_2 (T) \qquad (2)$$

The rate constants k were also determined according to an integral reaction model, but the differences with the differential one used here were insignificant.

The results of similar experiments, carried out at 480°C are given in fig. 5-5. Here the benzene formation rate is also proportional to the toluene concentration, but the toluene conversion rate is not simply first order in toluene. The non-selective reaction can be described with a Langmuir-Hinshelwood model:

$$-\left(\frac{d(T)}{dt}\right)_{\text{non-selective}} = \frac{k_1 (T)}{1 + k_3 (T)} \qquad (3)$$

Essentially, eq. (1) is equal to eq. (3) but with $k_3 = 0$. Equation (2) remains valid at this temperature. By varying the reaction temperature the energies of activation for k_1 and k_2 were determined. For the reaction rate constants we took the values obtained by extrapolation to (T) = 0 ensuring that the first order reaction model is valid. The Arrhenius plot is given in fig. 5-6. It follows that for both reactions the energy of activation is approx. 40 kcal.mole^{-1} in the 430-445°C region, and decreases to 15 kcal.mole^{-1} in the 500-520°C region.

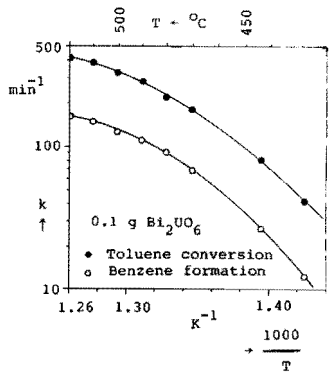

Fig. 5-6 Arrhenius plot for the toluene oxidation; pulse system

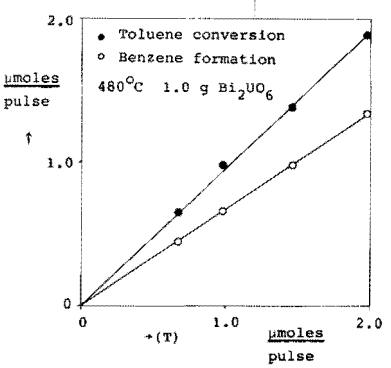

Fig. 5-7 Reaction rates as a function of the toluene inlet concentration (T); pulse system

In chapter 3 we remarked that the interpretation of the results would be difficult at high degrees of conversion because a gradient in oxygen content over the bed would occur. From the results obtained with 0.1 g of bismuth uranate we know that under the given conditions region B extends from a degree of reduction of 2% up to 10%. We can conclude that the B region reaction rates may also be determined at high conversions, provided that the first part of the oxidant is not reduced beyond 10%, while the last part must have attained region B. Experiments carried out with 1.0 g of oxidant showed that within a small range the reaction rates were indeed constant. We were therefore able to determine the B-reaction rates at high conversions as well, and consequently with greater accuracy.

The results of experiments with 1 g of Bi_2UO_6 are given in fig. 5-7. The first order parallel model applies. The dependence of the contact time on the reaction rates was measured by varying the amount of oxidant in the reactor. Results are given in fig. 5-8, and they support the first order model. The rate constants were also determined at different temperatures and an Arrhenius plot was constructed, shown in fig. 5-9. The apparent energy of activation for the toluene conversion is 30 kcal.mole^{-1} while that for the benzene formation declines from 55 at 420°C to 30 kcal. mole^{-1} at 480°C.

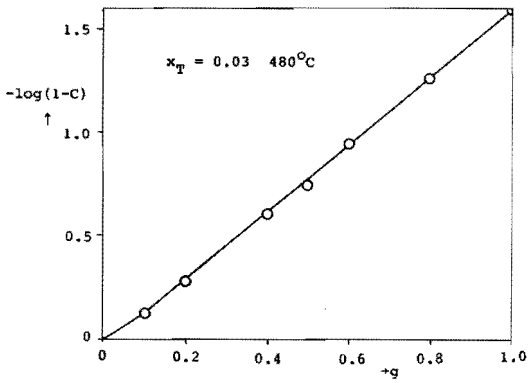

Fig. 5-8 -log(1 - Conversion) as a function of the amount of bismuth uranate in the reactor; pulse system

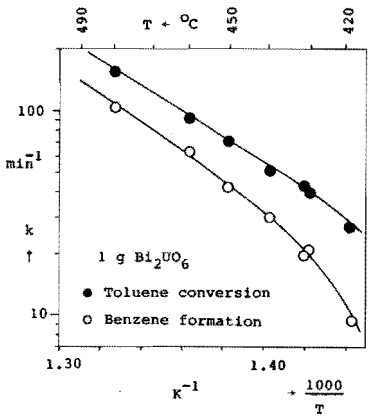

Fig. 5-9 Arrhenius plot for the toluene oxidation; pulse system

5.1.3. Region C

In region C, which begins at a degree of reduction of about 0.10 all reaction rates decline. In pulse experiments a very great number of pulses is required to attain this degree of reduction. Therefore, we investigated the reaction at high values of degree of reduction in the flow system and in the thermobalance only.

5.2 Flow experiments

The experiments in the flow reactor were carried out under the conditions given in table 5-2. The rather low sensitivity of the analysis system did not allow using toluene mole fractions lower than 0.02.

Table 5-2. Reaction conditions during flow experiments

gas flow	:6-25 $cm^3.min^{-1}$	amount of Bi_2UO_6	:0.1-0.5 g
reaction pressure	:atmospheric	particle size	:1.7-2.4 mm
reaction temperature	:460-500°C	toluene mole fraction	:0.02-0.18

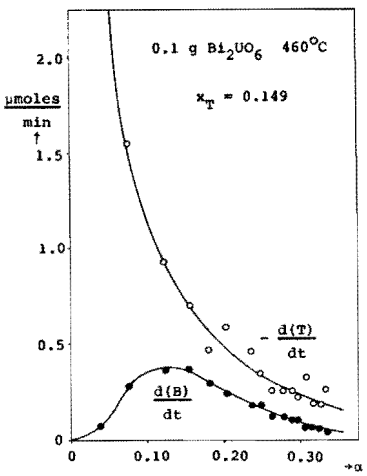

Fig. 5-10 Reaction rates as a function of the degree of reduction of Bi_2UO_6 in the flow reactor

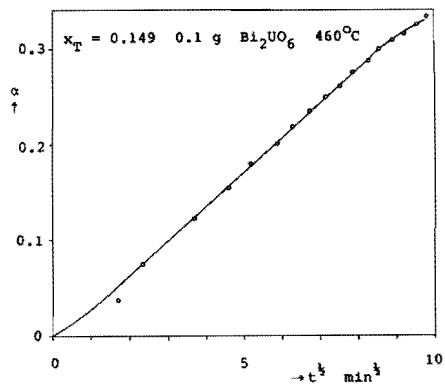

Fig. 5-11 Degree of reduction of bismuth uranate as a function of the square root of time; flow reactor

The results of a typical experiment are given in fig. 5-10. They appear to differ greatly from those obtained under pulse conditions. A division into three definite regions is now impossible. There is a continuing decrease in toluene conversion rate, while the rate of benzene formation has a maximum at a higher degree of bulk reduction value than during pulse experiments. Regions with constant activity are absent. Furthermore, the reaction rates are considerably lower. The reproducibility of the flow experiments is not too good. In chapter 4 we already stated that this may be due to incomplete reoxidation of the bismuth uranate after an experiment. If bismuth uranate is strongly reduced, the bismuth metal particles formed during the reaction fuse to large conglomerates, which are difficult to reoxidize. As a result, the regenerated sample may still contain free bismuth metal or bismuth oxide, resulting in an error in the calculated degree of reduction. Further, incomplete reoxidation of Bi-metal implies that the Bi/U ratio in the bismuth uranate has become smaller than 2, which can affect selectivity. This effect is absent in the experiments carried out with the pulse system or the thermobalance, since in these systems we performed every run with a new sample of the same batch of bismuth uranate. Errors in the degree of reduction may also stem from the difficulty in defining a good starting time of the reaction, as was discussed in chapter 3. A systematic decrease in activity or selectivity with the number of reaction cycles in the flow system could not be observed. Although the form of the curves of which fig. 5-10 gives an example is not straightforward, it appears that if the degree of reduction of the oxidant is plotted against the square root of the reaction time, a straight line is obtained (fig 5-11).This phenomenon will be accounted for in the discussion of this chapter, where mathematical relations for the rate of reduction are derived.

At gas velocities greater than 40 $cm^3.min^{-1}$ per g of Bi_2UO_6 the influence of the gas flow on the reaction rates is negligible. Below 40 $cm^3.min^{-1}$ a decrease in reaction rate is observed. Under the latter conditions the toluene conversion becomes so high that the toluene concentration may not be considered constant over the fixed bed, which lead to a drop in the observed reaction rates.

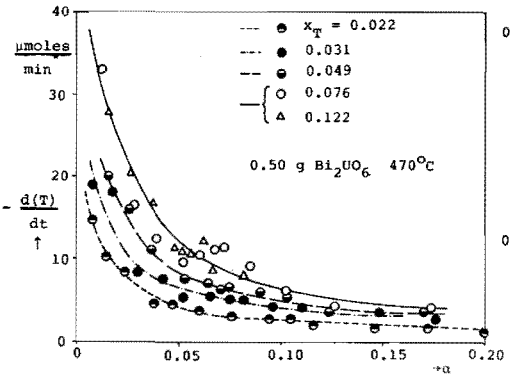

Fig. 5-12 Rate of toluene conversion as a function of the degree of reduction; flow reactor

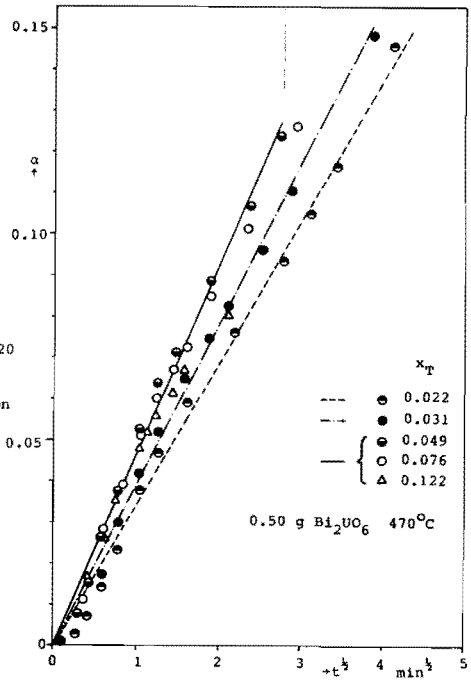

Fig. 5-15 Degree of reduction of bismuth uranate as a function of the square root of time; flow reactor

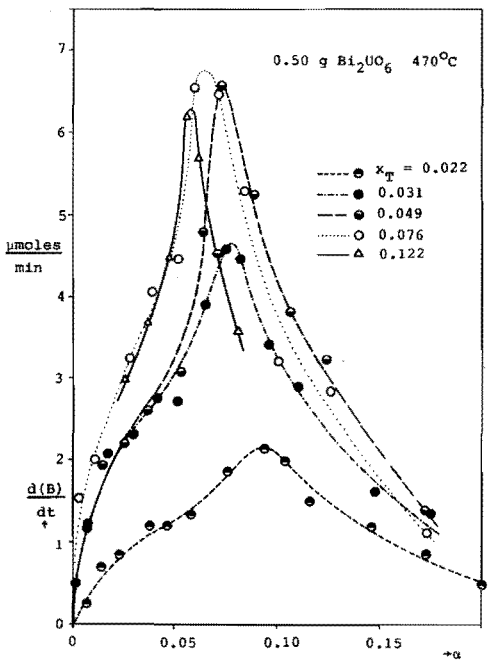

Fig. 5-13 Rate of benzene formation as a function of the degree of reduction; flow reactor

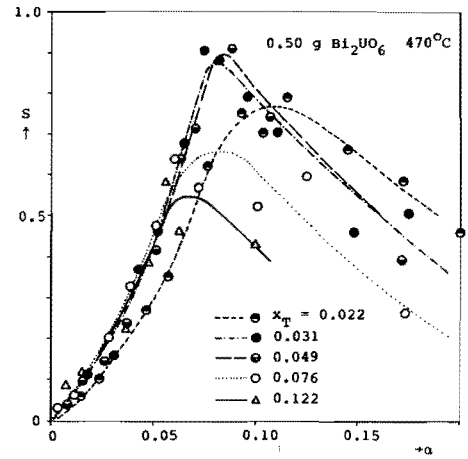

Fig. 5-14 Selectivity as a function of the degree of reduction of bismuth uranate; flow reactor

All kinetic data to be discussed in the following are obtained at gas flows higher than 40 $cm^3.min^{-1}$.

Within the experimental error, no influence on the reaction rates was observed when the particle size was reduced tenfold.

Fig. 5-12 shows the influence of the toluene concentration on the conversion rate of toluene. It is seen that the conversion rate becomes zero order in toluene at a mole fraction $x_T > 0.07$. Fig. 5-13 gives the rate of formation of benzene. The selectivities are represented in fig. 5-14. The highest selectivities appear to be obtained with $x_T = 0.04$. In fig. 5-15 the degree of reduction α has been plotted against the square root of the time for various toluene mole fractions. Straight lines passing through the origin are obtained, hence:

$$\alpha = k\, t^{\frac{1}{2}} \qquad (4)$$

Since:

$$\alpha = \frac{O_o - O_t}{O_o} \qquad (5)$$

O_o: number of oxygen atoms present at t=0

O_t: number of oxygen atoms present at time=t

it follows that:

$$-\frac{dO_t}{dt} = \frac{k^2 O_o}{2\alpha} = \frac{k^2 O_o^2}{2} \cdot f(O_t) \qquad (6)$$

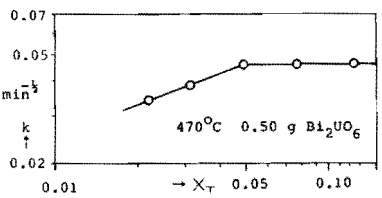

Fig. 5-16 Reduction rate constant as a function of the toluene mole fraction, logarithmic scales; flow reactor

This relation has the form of a reaction rate equation with rate constant $k^2 O_o^2/2$. Assuming that the influence of the toluene concentration on this rate constant can be described by saying that this rate constant is proportional to $(x_T)^n$ in which n is the order in toluene of the reduction reaction, one obtains:

$$\frac{n}{2} \log x_T = C + \log k \qquad (7)$$

n can be found from a plot of log k versus log x_T given in fig. 5-16, and is 0.7 for $x_T < 0.05$, and zero for $x_T > 0.05$.

Within the experimental conditions the effect of the temperature on the selectivity is small. There is a slight tendency towards a higher selectivity at higher temperatures. The effect of the temperature is investigated in more detail in the thermobalance experiments.

5.3 Thermobalance experiments

Since the relations for -dO/dt are much less ambiguous than those for -d(T)/dt or d(B)/dt, we devoted particular attention to the former reaction rate. To investigate -dO/dt, the thermobalance is more suited than the flow reactor system. The degree and the rate of reduction of Bi_2UO_6 can be measured accurately and continuously, both at the high toluene concentration required in the flow apparatus and at the lower concentrations used during pulse experiments. The reaction conditions are given in table 5-3.

Table 5-3 Reaction conditions during thermobalance experiments

gas flow	:160 $cm^3.min^{-1}$	amount of Bi_2UO_6	:22 mg
reaction pressure	:atmospheric	particle size	:<0.15 mm
reaction temperature	:450 - 520°C	toluene mole fraction	:0.003-0.086

Since in the thermobalance the gases pass over and not, as in a tubular reaction, through the fixed bed of oxidant, the occurrence of physical limitations is not excluded. However, the gas flow proved to have no effect on the reaction rates at values higher than 160 $cm^3.min^{-1}$. Neither enlarging the particle size by a factor 10, nor enlarging the thickness of the layer of Bi_2UO_6 in the sample boat by a factor 2 had any influence.

A possible source of error in the determination of the degree of reduction of the oxidant is the adsorption of hydrocarbon or the formation of "coke" on the surface. If these effects occur, too high a weight of the sample is measured, resulting in too low a value for α. A C-H-analysis, carried out on a sample of Bi_2UO_6 that was completely reduced in the thermobalance, showed that 0.9 wt% of carbon and 0.07 wt% of hydrogen were present, corresponding to an error in α of 7%. In the following this error will be

neglected, since we usually work with much lower degrees of reduction.

The effect of the toluene concentration is shown in fig. 5-17. At toluene mole fractions of 0.0030 and 0.0055 three regions are distinguished just as during pulse experiments: a rapid decline in reduction rate at low α resembling region A of the pulse experiment, followed by a region in which the rate remains constant, and a final region in which the rate declines once again. At $x_T > 0.02$ the rate of oxygen depletion declines continuously, the curve with $x_T = 0.0084$ being an intermediate case.

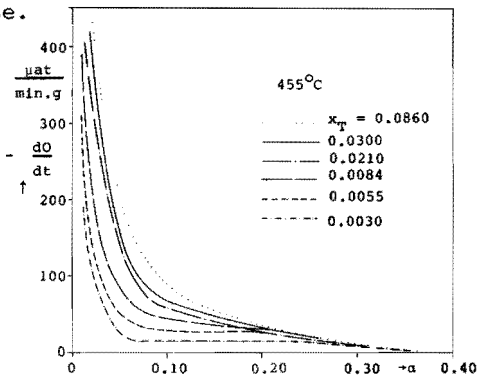

Fig. 5-17 Reduction rates as a function of the degree of reduction; thermobalance

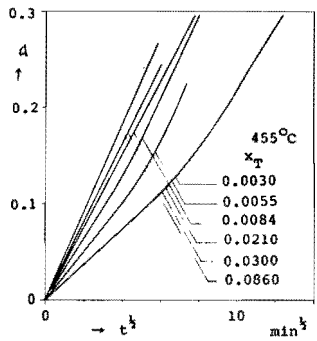

Fig. 5-18 Degree of reduction as a function of the square root of time; thermobalance

The curves of α plotted versus $t^{\frac{1}{2}}$ are depicted in fig. 5-18. Evidently the relation $\alpha = k\, t^{\frac{1}{2}}$ is obeyed up to $\alpha \simeq 0.30$ at higher toluene concentration, but at lower toluene mole fraction the expression holds good only to $\alpha \simeq 0.10$. The reaction order n can be calculated according to relation (8). A plot of log k versus log x_T is given in fig. 5-19. It follows that n is approx. 1 for low x_T and declines to 0.2 at higher x_T. This is in good agreement with the data from the flow experiments. If we plot the reaction rate in the region of constant activity (as obtained from the experiments with low x_T) against x_T, a curve is obtained shown in fig. 5-20. A straight line drawn through the first two points and the origin, indicates that here the reaction is first order in toluene. Thus we see that at these low toluene concentrations the reaction remains first order in toluene for α between 0 and 0.30, in spite of the fact that in this range a change in the kinetics occurs, as follows from fig. 5-17. From the latter figure

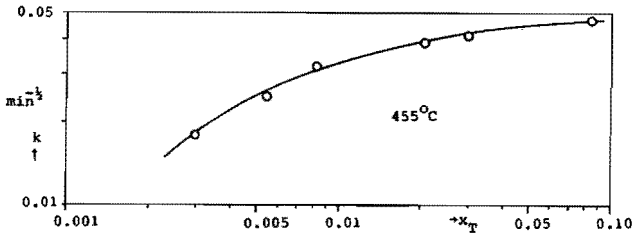

Fig. 5-19 Reduction rate constant as a function of the toluene mole fraction, logarithmic scales; thermobalance

it is seen that n becomes very low at $\alpha > 0.30$. The effect of the toluene temperature was studied at toluene mole fractions of 0.003 and 0.030. In fig. 5-21 the rates are given as a function of T for the lower toluene concentration. The three regions are clearly distinguished, and the region of constant activity appears to extend to a higher degree of reduction at the higher reaction temperature.

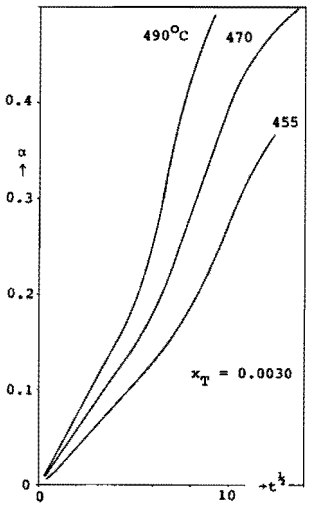

Fig. 5-22 Degree of reduction of bismuth uranate as a function of the square root of time

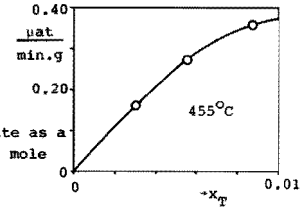

Fig. 5-20 Reduction rate as a function of the toluene mole fraction, $\alpha > 0.10$

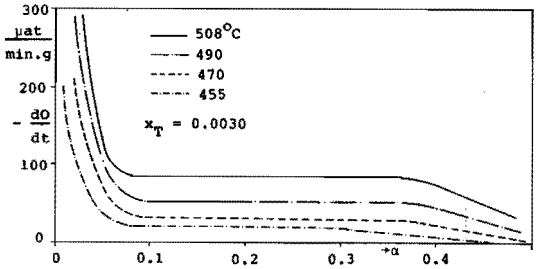

Fig. 5-21 Reduction rates as a function of the degree of reduction; thermobalance

Up to $\alpha \simeq 0.10$ the reaction can be described by eq. (4) (fig. 5-22). We already saw that the reaction rate equation has the form:

$$\frac{dO}{dt} = \frac{k^2 O_o}{2\alpha} = \frac{k^2 O_o^2}{2} \cdot f(O_t) \qquad (6)$$

$\frac{k^2 O_o^2}{2}$ is the rate constant and may be written in the form:

$$\frac{k^2 O_o^2}{2} = k_o \, e^{-E/RT} \qquad (8)$$

and therefore:

$$2 \log k = C - \frac{E}{2.3\ RT} \qquad (9)$$

Using eq. (9) we calculated an apparent energy of activation of 26 kcal.mole^{-1}, for $\alpha < 0.10$. From the reaction rates in the region $0.10 < \alpha < 0.30$ an energy of activation of 34 kcal.mole^{-1} was found (fig. 5-23). It is emphasized that these energies of activation apply to the rate of oxygen depletion, and not to that of toluene conversion. Recalculating the data obtained in the pulse experiments, we found for the rate of oxygen depletion an energy of activation of about 30 kcal.mole^{-1}.

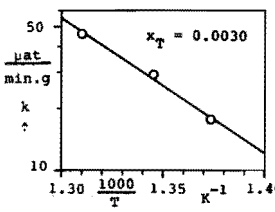

Fig. 5-23 Arrhenius plot for the rate of reduction of bismuth uranate

At $x_T = 0.030$ the picture is different. Eq. (4) is obeyed up to $\alpha = 0.30$ (fig. 5-24). The apparent energy of activation is approx. 50 kcal.mole^{-1} at 450°C, and increases to 60 kcal.mole^{-1} at about 480°C (fig. 5-25, circles).

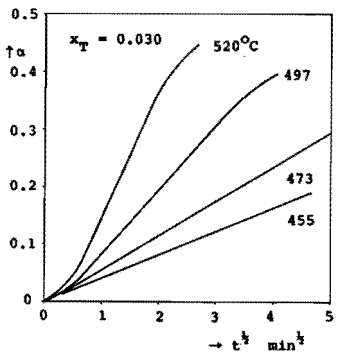

Fig. 5-24 Degree of reduction of bismuth uranate as a function of the square root of time; thermobalance

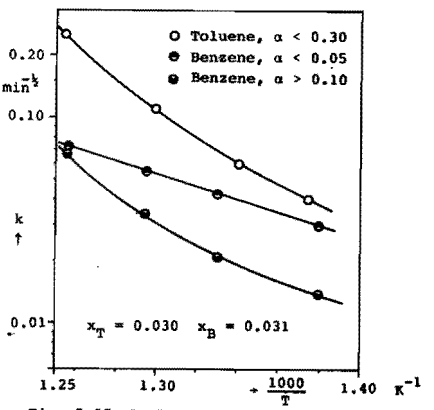

Fig. 5-25 Arrhenius plot for the rate of reduction of bismuth uranate; thermobalance

The effect of the specific surface area of the solid was studied at x_T = 0.0030 only. Results are represented in fig. 5-26. It is clear that the reaction rates in the constant activity region expressed per square metre of bismuth uranate surface area are approximately equal. However, this region extends to $\alpha \simeq 0.40$ with the samples having a high specific surface area, while it ends at about 0.12 with the sample having a low area.

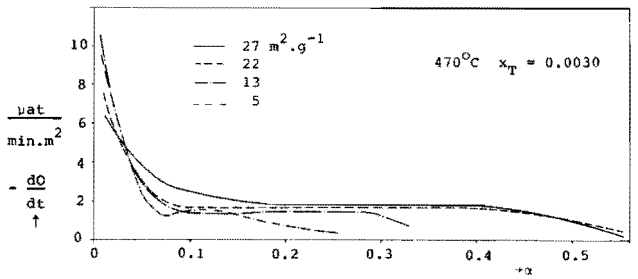

Fig. 5-26 Rate of reduction of bismuth uranates with different surface areas; thermobalance

The results, obtained for the reduction of bismuth uranate by toluene have been summarized in table 5-4.

Table 5-4 Reduction of bismuth uranate by toluene under flow conditions

Mole fraction	Degree of reduction	Kinetic model	Order in toluene	Activation energy
< 0.005	$\alpha<0.10$	$\alpha=k\ t^{\frac{1}{2}}$	1	26 kcal.mole^{-1}
	$\alpha>0.10$	$\alpha=k\ t$	1	34
> 0.02	$\alpha<0.30$	$\alpha=k\ t^{\frac{1}{2}}$	0.2	50-60

5.4 Oxidation of benzene

The oxidation of benzene was studied for two reasons: (a) to investigate the consecutive oxidation of benzene formed from toluene, and (b) as a model reaction for the non-selective oxidation of the aromatic nucleus.

We already noted that under pulse conditions the oxidation of benzene is negligible at $\alpha > 2\%$. However, in the flow system the bismuth uranate behaves differently, and some benzene is oxidized at a higher degree of reduction as well. Since the only

reaction products are CO_2 and H_2O the benzene reaction rate is always proportional to the rate of reduction of bismuth uranate. Therefore it is sufficient to investigate the latter reaction rate in the thermobalance.

Fig. 5-27 gives the degree of reduction as a function of $t^{\frac{1}{2}}$ for a number of temperatures. Equation (4) is obeyed up to $\alpha = 0.05$. After that the reduction rate declines and at $\alpha > 0.10$ a region follows in which $\alpha = k\, t^{\frac{1}{2}} + C$. From these results an energy of activation of 22 kcal.mole^{-1} can be calculated for the region $\alpha < 0.05$. At $\alpha > 0.10$ the energy of activation increases from 50 kcal.mole^{-1} at 450°C to approx.65 at 480°C. An Arrhenius plot, in which the experimental results for the oxidation of toluene have been given as well, is represented in fig. 5-25.

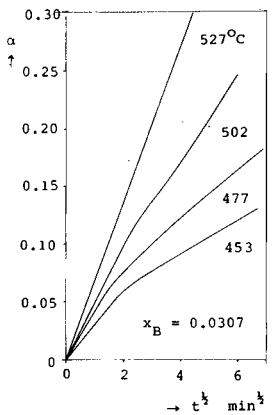

Fig. 5-27 Degree of reduction of bismuth uranate as a function of the square root of time; thermobalance

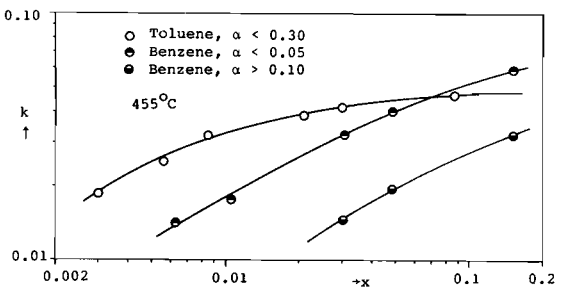

Fig. 5-28 Reduction rate constants as a function of mole fraction, logarithmic scales; thermobalance

The order of the reaction was determined according to eq. (7). A plot of log k versus log x_B is given in fig. 5-28. This picture also includes the data for the toluene oxidation, already given in fig. 5-19 (circles). The reaction order is approx. 1 at $x_B < 0.05$, and decreases slightly at higher mole fractions. n is equal for both regions of α.

Our toluene oxidation experiments were carried out under differential conditions. Therefore, the consecutive oxidation of benzene may be neglected. However, the results obtained for the oxidation of benzene indicate that the consecutive reactions must be reckoned with when large conversions are used.

We may also consider the oxidation of benzene as model reaction for the oxidation of the aromatic nucleus, hence for

the non-selective oxidation of toluene. The selectivity is, in fact, the ratio of side chain oxidation to oxidation of the aromatic nucleus. It can be seen from fig. 5-25 and 5-28 that this ratio should have a maximum for low toluene concentrations and high reaction temperatures, which is supported by our experimental data.

5.5 Discussion

5.5.1 Theory of gas-solid reactions

The demethylation of toluene by bismuth uranate has so far been described as an oxidation reaction in which bismuth uranate acts as the oxidant. However, the process can also be described as a reduction of bismuth uranate by toluene. Hence it may be worthwhile to apply the kinetic relations derived for the reduction of oxides and mixed oxides to our reaction.

Experimental data on this subject are not always straightforward. Even for an extensively investigated reaction of great commercial importance such as the reduction of iron ore, the results obtained by different authors are contradictory (1). This stems from the fact that the reaction is composed of several steps, each of which may influence the overall reaction rate, while the composition and texture of the surface, which are difficult to investigate also play an important part.

In the following, we shall discuss a number of kinetic models applicable to gas-solid reactions and at the end of this discussion we shall consider to what extent the information obtained is applicable to our system.

Let us first consider the catalytic reaction of a gaseous substrate A on the surface of a non-porous solid B:

$$A(g) \xrightarrow{B(s)} P(g)$$

The overall process can be divided into three consecutive steps, viz.

(a) diffusion of A from the gas bulk through the gas film layer to the surface;

(b) chemical reaction at the surface; this step may be subdivided

into: adsorption of A, chemical reaction, desorption of P; (c) diffusion of P through the gas film to the gas bulk. Which of these steps is actually rate-determining can be derived from experimental work and the following considerations. If the chemical reaction is rate-limiting, the order of the reaction is usually one or higher at low substrate concentrations, and tends towards a lower order at high concentrations. The energy of activation will lie between 10 and 40 kcal.mole^{-1}. The reaction rate is independent of the gas velocity at constant time. Whether step (a) or (c) is rate-determining is usually rather difficult to establish. If one of these steps controls the reaction rate, i.e. film diffusion limitation is operative, one finds an energy of activation of the order of 1 kcal.mole^{-1}, while the reaction rate increases with the gas velocity. Film diffusion limitation usually occurs at high reaction temperatures and low gas velocities. Its occurrence can be established by calculating the drop in partial pressure of the substrate over the gas film around the solid. If this is low as compared with the bulk substrate partial pressure, film diffusion limitation can be ruled out. The partial pressure is found from:

$$\Delta p = p_g - p_s = \frac{\phi_m}{k_{gm}} \qquad (14)$$

In this relation p_g is the substrate partial pressure in the gas bulk in N.m^{-2}, p_s that at the surface, ϕ_m the mass flux of the substrate through the film in kg.m^{-2}.sec^{-1} and k_{gm} the mass transfer coefficient in sec.m^{-1}. k_{gm} can be calculated according to various equations, the most reliable of which seem to be those of Chu et al. (2) and of Petrovic and Thodos (3).

If the solid B is porous, the situation becomes more complex. The diffusion of A through the pores of the particle to the reaction surface has now also to be taken into account.

If the reaction rate at the surface is relatively low, the diffusion through the pores will usually keep up with the chemical reaction. But when the chemical reaction rate increases, the concentration of substrate will decrease along the length of the pores and will become markedly lower than in the gas bulk, influencing the observed rate of reaction.

Eventually, the diffusion of A through the gas film surrounding the particle becomes rate-limiting. In the case of pore diffusion limitation the apparent activation energy has half the value of that when the chemical reaction is rate-controlling, while in the case of film diffusion limitation the energy of activation is of the order of 1-2 kcal.mole^{-1}. Since the probability that pore diffusion is the rate-limiting step increases with the particle size, a simple experiment to check whether pore diffusion limitation is operative, is to examine whether variation in particle size has any influence on the rate of reaction.

A treatise on the theory of pore diffusion is given by Satterfield and Sherwood (4). They describe this phenomenon in terms of an effectiveness factor η, defined as the ratio between the measured reaction rate to the hypothetical one, should the internal surface be fully effective. To calculate η one first has to determine D_{eff}, the effective diffusion coefficient of the substrate through the pores:

$$\frac{1}{D_{eff}} = \frac{1}{D_{knud}} + \frac{\tau_p}{D_{1,2}\varepsilon_p} \qquad (15)$$

in which D_{knud} represents the Knudsen diffusion coefficient, cm^2.sec^{-1}, τ_p the tortuosity factor (for cylindrical pores equal to 2), ε_p the porosity of the particle, and $D_{1,2}$ the free gas diffusion coefficient of substrate 1 in a mixture of gases 1 and 2. D_{knud} follows from:

$$D_{knud} = \frac{2\ r_p}{3} \left(\frac{8RT}{M} \right)^{\frac{1}{2}} \qquad (16)$$

in which r_p is the pore radius in cm, R the gas constant and M the molecular weight. For the calculation of $D_{1,2}$ several relations exist. A very convenient one is that of Slattery and Bird (5). Knowing D_{eff} the Thiele modulus ϕ_{Th} can be found according to:

$$\phi_{Th} = r_o \left(\frac{k_v}{D_{eff}} \right)^{\frac{1}{2}} \qquad (17)$$

in which r_o is the particle radius in cm, and k_v the rate constant of the chemical reaction in sec^{-1}. Usually, k_v is unknown and has to be eliminated with the following relation, valid for a first order reaction:

$$- \frac{dn}{dt} = k_v \, V_c \, c_s \, \eta \qquad (18)$$

where V_c is the catalyst volume in cm^3, c_s the substrate concentration in $mol.cm^{-3}$, $\frac{dn}{dt}$ the number of moles converted per second. From (17) and (18) we obtain:

$$\phi_{Th}^2 \, \eta = \frac{r_o^2}{D_{eff} c_s} \left(- \frac{1}{V_c} \frac{dn}{dt} \right) \qquad (19)$$

For a spherical particle, involved in a first order reaction:

$$\eta = \frac{3}{\phi_{Th}} \left(\frac{1}{\tanh \phi_{Th}} - \frac{1}{\phi_{Th}} \right) \qquad (20)$$

From equations (19) and (20) η can be found. Satterfield (4) gives figures in which η is plotted against $\phi_{Th}^2 \, \eta$. Since the latter function can be calculated with eq. (19), η can easily be found.

So far we have dealt with catalytic reactions in which the solid remains unchanged. It is evident that the reduction of an oxide does not proceed according to this scheme, since in the latter type of reaction the solid is actually a reactant, and changes in the solid must be taken into consideration. Therefore we will now focus our attention to the reaction:

$$A(g) + B(s) \rightarrow P(g)$$

The theory of pore and film diffusion limitations given above is valid for this reaction type as well, but one has to remember that during the process the solid B is gradually consumed, leading to a decrease in surface area and reaction rate. It can be derived that for a spherical particle:

$$\frac{t}{\tau} = 1 - (1 - f)^{1/3} \quad \text{or:} \quad \frac{df}{dt} = \frac{3}{\tau^3}t^2 - \frac{6}{\tau^2}t + \frac{3}{\tau} \qquad (21)$$

in which τ is the time required for total conversion of B, and f the fraction of B converted. This equation is commonly known as the "shrinking core" relation, and gives a good description of many reactions of the type under consideration. When gas film resistance is rate-controlling, one obtains:

$$\frac{t}{\tau} = 1 - (1 - f)^{2/3} \qquad (22)$$

Equations (21) and (22) are valid for spherical particles only. For infinite flat plates, eq. (21) becomes:

$$\frac{t}{\tau} = f \quad \text{or:} \quad \frac{df}{dt} = k \qquad (23)$$

while for cylindrical particles:

$$\frac{t}{\tau} = 1 - (1 - f)^{\frac{1}{2}} \quad \text{or:} \quad f = -\frac{t^2}{\tau^2} + 2\frac{t}{\tau} \qquad (24)$$

This illustrates that now the geometry of the solid has a profound influence on the reaction kinetics.

The picture grows even more complicated for reactions of the type:

$$A(g) + B(s) \rightarrow P(g) + Q(s)$$

corresponding most closely to the reduction of an oxide by a gaseous substrate. If the reaction product Q forms a non-porous layer of solid round a core of unconverted B, the substrate has to move through the layer of Q to react at the surface of B, while the reaction product P has to move back to the gas bulk. This type of diffusion, to be called product layer diffusion, is likely to control the overall rate of the reaction. It can be derived that in that case:

$$\frac{t}{\tau} = 1 - 3(1 - f)^{2/3} + 2(1 - f) \quad \text{or:}$$

$$\frac{df}{dt} = \frac{(2\tau)^{-1}}{(1 - f)^{-1/3} - 1} \tag{25}$$

for a spherical particle, and:

$$f = k\, t^{\frac{1}{2}} \quad \text{or:} \quad \frac{df}{dt} = k' t^{-\frac{1}{2}} \tag{26}$$

for an infinite flat plate. This is the "parabolic law" applicable to the oxidation of metal surfaces.
A reaction controlled by product layer diffusion usually has a low energy of activation.

Should the reaction at the surface of the unreacted core of B be the rate-determining step, relation (21) remains valid. If the gas film diffusion controls the reaction rate, the picture is not different from that for a non-changing particle, and eq. (23) applies. For the case that both product layer diffusion and chemical reaction are rate-determining, relations have been derived by Massoth et al. (6), and by Seth and Ross (7). Comparing the relations (21), (22) and (25) it is evident that it is difficult to decide whether a reaction is controlled by chemical reaction, product layer diffusion or gas film diffusion simply on the basis of a plot of f versus t in one or another form. The reaction order and the effects of temperature and particle size variation have always to be taken into account.

When the solids B and Q are porous, the diffusion through the pores has to be added to the effects already mentioned. Since industrial gas-solid reactions are usually carried out with relatively large particles, so that pore diffusion limitations are likely to occur, this type of reaction has had the attention of a great number of authors (8, 9, 10). A general model has recently been developed by Sohn and Szekely (11). They found that in the case of rapid diffusion and slow chemical reaction, eq. (21) becomes operative, whilst if pore diffusion is rate-limiting, eq. (25) holds. The intermediate cases were solved numerically and represented in dimensionless form. On the other hand, if the

absence of diffusional limitations can be established, either experimentally or with equations (19) and (20), the porous particle can be dealt with as a non-porous one.

Let us now return to the reduction of bismuth uranate, and see which of the relations given above may be applied to the reaction. Bismuth uranate is porous, hence the occurrence of pore diffusion limitation must be investigated. The absence of this type of limitations follows from a number of arguments.

1. Calculations according to eq. (19) yield 0.55 for $\phi_{Th}^2 \eta$ indicating that the effectiveness factor is very close to 1.
2. The reaction rate is unaffected by variation in particle size.
3. The observed energy of activation is relatively high.

Film diffusion limitations can be ruled out on the following grounds:

1. Calculations according to eq. (14) show that the drop in partial pressure over the gas film is negligible.
2. The energy of activation is much higher than is to be expected for a reaction controlled by film diffusion.

These results reduce the number of relations possibly applicable to our reaction to eq. (21) and (25) or one of their equivalents for a non-spherical particle. However, none of these equations constitute an appropriate description of the experimental data.

5.5.2 Models incorporating diffusion through the lattice

In chapter 4 we have dealt with the reduction of bismuth uranate from a qualitative point of view, on the basis of the products formed during the reaction. It appeared that the reaction occurs at the surface of the solid under the formation of metallic bismuth and a uranium-rich phase, and that a Bi_2UO_6-like structure is restored by diffusion of oxygen ions through the lattice to the surface.

Let us assume that the number of active sites at the surface is controlled by the number of surface oxygen ions that participate in the reaction. It must be noted that not all oxygen atoms can react; under our conditions Bi_2UO_6 cannot lose more than 4 of its 6 oxygen atoms. The oxygen removed in the course of the reaction is replenished by diffusion from the bulk to the surface. First,

the case will be considered that the diffusion is fast in comparison with the chemical reaction. Then the actual surface oxygen concentration is equal to that in the bulk:

$$(O)_{surf} = (O)_{bulk} \qquad (27)$$

If the oxygen concentration is high, the reaction will be first order in substrate concentration (T), but zero order in participating oxygen (O) and:

$$-\frac{d(O)}{dt} = k\ (T) \quad \text{or: } \alpha = k\ t \qquad (28)$$

If the concentration of oxygen becomes low in comparison with the substrate concentration, the reaction is first order both in substrate concentration and in (O), hence:

$$-\frac{d(O)}{dt} = k\ (T)\ (O)_{surf} = k\ (T)\ (O)_o e^{-k(T)t} \qquad (29)$$

$(O)_o$ represents the concentration of removable oxygen at $t = 0$. The degree of conversion f of the solid follows by integration of eq. (29):

$$f = 1 - e^{-k(T)t} \qquad (30)$$

f is related to the degree of reduction of the solid as defined in eq. (5) by:

$$f = \frac{\alpha}{\alpha_\infty} \qquad (31)$$

in which α_∞ represents the degree of reduction at infinite t.

Although at first sight these equations are a good description of the region at constant activity as observed under pulse conditions and of the continuous decrease in reduction rate in the flow experiments, they do not explain the differences between the reaction rates in pulse and flow experiments, the high activation energy or the effect of crystallite size variation. It appears that the rate of oxygen diffusion through the lattice

plays a role in the observed kinetics.

For a more quantitative description of such a process, the kinetics of both the chemical reaction step and the oxygen diffusion step should be combined. This has been done by Schuit et al. for the reduction of bismuth molybdate by 1-butene (12). The authors make the following assumptions:

1. The physical properties of the solid (surface area, particle size, diffusion coefficients) do not change during the reaction.
2. The solid is semi-infinite with one boundary plane at which the reaction takes place.
3. The diffusion occurs in one direction only, perpendicular to the boundary plane.
4. The rate of the chemical reaction at the surface is equal to that of the diffusion from the bulk to the surface.

They found the following expression:

$$f = \frac{S\rho D}{k\lambda} \left\{ e.erfc\left(\frac{k\lambda t^{\frac{1}{2}}}{D^{\frac{1}{2}}}\right) - 1 + \frac{2k\lambda t^{\frac{1}{2}}}{\pi^{\frac{1}{2}} D^{\frac{1}{2}}} \right\} \qquad (32)$$

in which f is the degree of conversion of the solid, S the specific surface area in $cm^2.g^{-1}$, ρ the density in $g.cm^{-3}$, k a rate constant in sec^{-1}, λ a so-called jump distance in cm, of the order of the lattice constant, D the diffusion coefficient of oxygen in the lattice, in $cm^2.sec^{-1}$, and t the reaction time in sec. Furthermore, e.erfc x is equal to $e^{x^2}(1 - erf\ x)$.

Equation (32) can be solved numerically. Between certain limits of t, it can be written in the approximative form:

$$f = -A + B\, t^{\frac{1}{2}} \qquad (33)$$

in which $A = \frac{S\rho D}{k\lambda}$ and $B = \frac{2S\rho D^{\frac{1}{2}}}{\pi^{\frac{1}{2}}}$

With this expression the authors calculated k and D for the reduction of bismuth molybdate.

The model of Schuit has two drawbacks:

a. The solid is visualized as a semi-infinite flat plate, which is justified by the assumption that the oxygen diffusion through the lattice occurs in one direction only.

b. It is assumed that at the surface $\frac{\delta c}{\delta t} = 0$, in other words, the rate of the chemical reaction is supposed to be equal to that of the diffusion from the interior.

In the following we shall develop a more general model for the reduction of an oxide by a gaseous substrate. We shall also include a chemical reaction step and a diffusion step, which are, however, not necessarily equal in rate, and we also assume the physical properties of the solid to remain constant.

We consider a spherical particle with radius a and a surface layer with thickness d, d being small as compared to a. The concentration of removable oxygen in the sphere is a function of r and t and will be named c (r, t) or c. We assume that in the surface layer a reaction takes place between the gas and the oxide, which is first order both in substrate concentration and in participating oxygen. We also assume that the oxygen concentration gradient over the layer is negligible. Oxygen atoms are removed from the surface layer by chemical reaction and replenished by diffusion from the bulk. The number of oxygen atoms M_1 removed per unit of time Δt from the surface layer is given by:

$$M_1 = 4\pi a^2 dk' c_o c \Delta t \qquad (34)$$

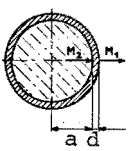

in which c_o is the substrate concentration, kept constant during the process, and k' a rate constant. The number of atoms M_2 transferred from the sphere to the layer is equal to:

$$M_2 = -4\pi a^2 D \left(\frac{\delta c}{\delta r}\right)_{r=a} \Delta t \qquad (35)$$

in which D is the diffusion coefficient. For the net oxygen transport we obtain:

$$\left(\frac{\delta M}{\delta t}\right)_{r=a} = 4\pi a^2 d \left(\frac{\delta c}{\delta t}\right)_{r=a} = -4\pi a^2 D \left(\frac{\delta c}{\delta r}\right)_{r=a} - 4\pi a^2 dkc \qquad (36)$$

with $k = k' c_o$.
The boundary condition now becomes:

$$\frac{\delta c}{\delta t} = -\frac{D}{d}\left(\frac{\delta c}{\delta r}\right) - kc \quad \text{at } r=a \text{ and } t \geqslant 0 \qquad (37)$$

For a spherical particle:

$$\frac{\delta c}{\delta r} = 0 \quad \text{at } r = 0 \text{ and } t \geqslant 0 \tag{38}$$

We assume c(r,0) to be equal to 1 and solve Fick's second law for a spherical symmetrical system:

$$\frac{\delta c}{\delta t} = D\left(\frac{\delta^2 c}{\delta r^2} + \frac{2\delta c}{r\delta r}\right) \quad 0<r<a \tag{39}$$

with boundary conditions (37) and (38) and initial condition c(r,0)=1 by the Laplace transform method *. Introducing the notation:

$$\tilde{c}(r,p) = \int_0^\infty e^{-pt} c(r,t)dt \tag{40}$$

equation (39) becomes:

$$p\tilde{c} - 1 = D\left(\tilde{c}'' + \frac{2}{r}\tilde{c}'\right) \quad 0<r<a \tag{41}$$

where c' and c" are the first and second derivatives to r of c(r,t), respectively. Equation (37) becomes:

$$-\frac{D}{d}\tilde{c}' = p\tilde{c} - 1 + k\tilde{c} \qquad r=a \tag{42}$$

Substituting $\tilde{c} = \frac{u}{r}$ in eq.(41) we obtain:

$$p\,u - r = D\,u'' \tag{43}$$

The solution of (43) with $q = \left(\frac{p}{D}\right)^{\frac{1}{2}}$ is:

$$u = Ae^{-qr} + \frac{r}{p} + Be^{+qr}$$

since for r = 0, u = 0 it follows that A + B = 0 and:

$$u = Ae^{qr} - Ae^{-qr} + \frac{r}{p} = Q \sinh qr + \frac{r}{p}$$

* Thanks are due to Ir.J.J.A.M.Brands for his help with these derivations.

hence:

$$\tilde{c} = Q \frac{\sinh qr}{r} + \frac{1}{p} \qquad (44)$$

By substitution of (44) in (42) for r = a it follows that:

$$-\frac{D}{d}\left(Qq\frac{\cosh qa}{a} - Q\frac{\sinh qa}{a^2}\right) = pQ\frac{\sinh qa}{a} + kQ\frac{\sinh qa}{a} + \frac{k}{p} \quad \text{or:}$$

$$Q\left\{-\frac{D}{d}\left(q\frac{\cosh qa}{a} - \frac{\sinh qa}{a^2}\right) - p\frac{\sinh qa}{a} - k\frac{\sinh qa}{a}\right\} = \frac{k}{p} \qquad (45)$$

With $p = Dq^2$ one obtains:

$$Q = \frac{k\,a}{p\left[\left(\frac{D}{da} - Dq^2 - k\right)\sinh qa - \frac{Dq}{d}\cosh qa\right]} \qquad (46)$$

(46) substituted in (44) gives for r = a:

$$\tilde{c}(a, p) = \frac{k \sinh qa}{p\left[\left(\frac{D}{da} - Dq^2 - k\right)\sinh qa - \frac{Dq}{d}\cosh qa\right]} + \frac{1}{p} \qquad (47)$$

Eq. (47) represents the Laplace transform of the concentration c at the surface of the sphere. By inversion of the Laplace transform it follows that:

$$c(a,t) = 2\,c(r,0) \sum_{n=1}^{\infty} \frac{\frac{kad}{D}\, e^{-D\beta_n^2 t}}{a^2d^2\beta_n^4 + a^2\beta_n^2\left(1+\frac{3d}{a} - \frac{2kd^2}{D}\right) - \frac{kad}{D}\left(1 - \frac{kad}{D}\right)} \qquad (48)$$

in which β_n are the roots of:

$$\tan a\beta = \frac{a\beta}{1 - \frac{kad}{D} + ad\beta^2} \qquad (49)$$

Eq. (48) gives the concentration of removable oxygen at the surface of the particle, $t \geqslant 0$. The amount of oxygen $\phi(t)$ present

in the sphere at $t \geqslant 0$ is given by:

$$\phi(t) = \int_0^a 4\pi r^2 c(r,t)dr$$

With Fick's second law it follows that:

$$\phi'(t) = 4\pi \int_0^a D \frac{\delta}{\delta r}(r^2 \frac{\delta c}{\delta r})\, dr = 4\pi D a^2 (\frac{\delta c}{\delta r})_{r=a} \qquad (51)$$

and with boundary condition (37):

$$\phi'(t) = -4\pi a^2 d(\frac{\delta c}{\delta t})_{a,t} - 4\pi a^2 dkc(a,t) \qquad (52)$$

By integration of eq. (52) we obtain:

$$\phi(t) = 8\pi a^2 dc(r,0)$$

$$\sum_{n=1}^{\infty} \frac{\frac{kad}{D}}{a^2d^2\beta_n^4 + a^2\beta_n^2(1 + 3\frac{d}{a} - 2\frac{kd^2}{D}) - \frac{kad}{D}(1 - \frac{kad}{D})} (\frac{k}{D\beta_n^2} - 1)e^{-D\beta_n^2 t} + A$$

in which A is a constant. Since at $t = \infty$, $\phi(t) = 0$, it follows that $A = 0$. At $t = 0, \phi(0) = \frac{4}{3}\pi a^3 c(r,0)$

The degree of conversion f is defined as: $f = \frac{\phi(0) - \phi(t)}{\phi(0)}$

and therefore:

$$f = 1 - \frac{6d}{a} \sum_{n=1}^{\infty} [\frac{k}{D\beta_n^2} - 1] \frac{\frac{kad}{D}}{a^2d^2\beta_n^4 + a^2\beta_n^2(1+3\frac{d}{a} - 2\frac{kd^2}{D}) - \frac{kad}{D}(1 - \frac{kad}{D})} e^{-D\beta_n^2 t} \qquad (53)$$

Relation (53) represents the degree of conversion of the solid as a function of time. It can be solved numerically, provided that the values of k, a, d and D are available. The values of the roots

β_n of equation (49) can be found using the computer procedure known as REGULA FALSI.

In a similar way the degree of reduction at the surface can be found:

$$f_s = 1 - \frac{c(a,t)}{c(a,0)} \qquad (54)$$

These relations are applicable to gas-solid reactions involving a chemical reaction step followed by internal diffusion of a reacting species through the lattice of the solid. Examples are the reduction of oxides by various substrates, the reduction of chlorides by hydrogen, but also the isotopic exchange of oxides. For the latter process a relation, similar to ours, was derived by Klier (13), valid for the case that oxygen in an oxide is exchanged with a given quantity of labelled gaseous oxygen. Our model would describe such exchange experiments if the concentration of the labelled oxygen in the gas phase was kept constant.

5.5.3 Application to the reduction of bismuth uranate

If we review our experimental data in the light of the models derived, the reduction of bismuth uranate by toluene can be visualized in the following way:

a. Under pulse conditions the small quantity of oxygen removed during a pulse can be replenished in the time interval between the pulses. The oxygen diffusion does not play a role in the reaction kinetics, and the concentration of oxygen at the surface is equal to or only slightly lower than in the bulk. First, the non-selective A-oxygen is rapidly consumed. Then the B-oxygen, participating in the more selective reaction, is removed, and eq. (28) is operative. A region of constant activity (region B) is observed, under conditions where in the flow system and the thermobalance a continuous decrease in activity is observed, with much lower reaction rates than in the pulse system. Thus the kinetics in this region B of the pulse experiments are those of the chemical reaction at the surface and are unaffected by the diffusion. When the surface oxygen concentration has decreased to much, eq. (28) loses its applicability and the reaction rates

decline (region C).

According to various authors the catalytic oxidation of hydrocarbons over oxide catalysts may be considered as a two-step reaction. In the first step the hydrocarbon is oxidized by the catalyst, and in the second the reduced catalyst is reoxidized by gaseous oxygen (Mars and Van Krevelen mechanism). Often the first step is rate-limiting. Since the rate determining step in the B-region of our pulse experiments is also the reduction of the solid surface, it is interesting to compare our kinetic data to those obtained by other authors for the catalytic air oxidation of toluene to e.g. benzaldehyde or benzoic acid. Some data are summarized in table 5-2.

Table 5-2 Kinetics of catalytic air oxidation of toluene

Authors	Catalyst	Kinetic Model	Activation Energy kcal.mole^{-1}	Ref.
Downie	V_2O_5	$r=\frac{k_a k_t (O)(T)}{k_a (O)+Nk_t (T)}$	k_a:26.4 k_t:29.4	(14)
De Jong	Bi_2UO_6	$r= k\ (T)$	34	Present work
Kumar	Ce/Mo-oxide	$r= k\ (T)$	29.2	(15)
Kumar	V_2O_5	$r= k\ (T)$	19.7	(16)
Popova	CuO	$r= k\ (T)$	22	(17)
Reddy	MoO_3	$r= k\ (T)$	23 *	(18)

* Calculated from Reddy's experimental data.

b. Under continuous flow conditions at low toluene concentration, the rate of diffusion can, more or less, keep up with the chemical reaction rate. After removal of the A-oxygen, already dealt with in the description of the pulse experiments, the activity is constant (eq. 28). Eventually the oxygen concentration becomes too low, and the observed rate of reaction declines. When the temperature is increased, the oxygen diffusion is accelerated more rapidly than the chemical reaction, which explains why the region of constant activity extends further at the higher temperature.

c. Under flow conditions at high toluene concentration the chemical reaction is enhanced, and now the diffusion rate enters the picture. Eq. (28) holds no longer, and the chemical-reaction plus diffusion model becomes operative. The concentration of oxygen at the surface is considerably lowered, and the reaction rate declines continuously. When the temperature is increased in this concentration range, a high energy of activation is observed (approx. 60 kcal.mole^{-1}) evidently due to the high activation energy of the oxygen diffusion. If we assume that the diffusion of the A-oxygen through the lattice is slower than that of the B-oxygen, although the former reacts more rapidly, we can also understand why at high toluene concentration, i.e. in the diffusion controlled regime, a definite A-region cannot be observed. Then the A-oxygen is consumed more slowly than the B-oxygen, and the regions A and B overlap. On the other hand, at low toluene concentration the rate of reduction of these A-oxygen atoms should also follow the chemical - reaction plus diffusion model (eq. (53)). When the particle size of the crystallites is reduced by using a bismuth uranate having a higher specific surface area, the region of constant activity extends up to a higher value of α, which is not surprising since now the oxygen atoms have to move a shorter distance to the surface, and the diffusion plays a minor role in the process.

To describe experimental data with eq. (53), four variables must be known, viz. the chemical reaction rate constant k, the particle radius a, the diffusion coefficient D and the thickness of the surface layer d. It is evident that with four variables a great number of experimental curves can be simulated. Therefore it is essential to estimate the parameters beforehand, possibly from other sources. Since under flow conditions at toluene mole fractions higher than 0.02 the reduction of bismuth uranate follows relation (33) (figures 5-11, 15, 18, 22, 24), we used the procedure described by Schuit (12) in order to find provisional values of k and D. In our case the constant A proved to be too small to determine k accurately.

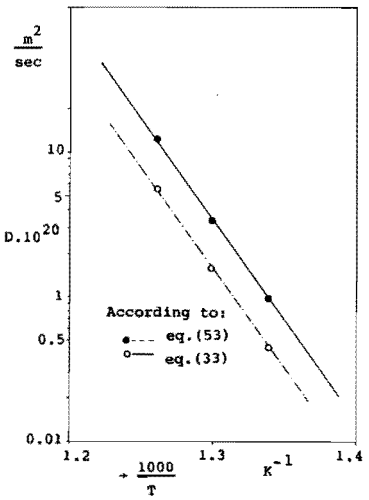

Fig. 5-29 Arrhenius plot for the diffusion coefficient of oxygen in bismuth uranate

The diffusion coefficient is $0.5 \cdot 10^{-20} m^2.sec^{-1}$ at 473°C. The energy of activation for the diffusion coefficient as determined from eq. (33) follows from figure 5-29 (circles) and has a value of 63 kcal.mole^{-1}. The average crystallite radius is 150 Å (see chapter 2). For the layer thickness d we chose a value of 5 Å, being the smallest cell parameter of Bi_2UO_6.

With these values for a, d and D we calculated the degree of conversion f as a function of the time t for various values of k.The final values of k, a, d and D were obtained by an iterative method*. In figures 5-30 and 5-31 some experimental curves are given together with the calculated points. Agreement is excellent. It can be seen that at low f the simulated curve hardly deviates from the relation $f = k\, t^{\frac{1}{2}}$. The energy of activation for D as obtained from the best fit is 63 kcal.mole^{-1} (fig. 5-29, dots).

The particle radius a and the surface layer thickness d that we used in our simulations are not known exactly. For that reason we also tried to fit the experimental curve with other values of a and d. It appeared that when d is increased at constant a and D, the rate constant k has to be reduced. The particle radius a and the diffusion coefficient D are related similarly. The model is much more sensitive to changes in a or D than in k or d.

* The help of Dr G.J.Visser in writing the computer program is gratefully acknowledged.

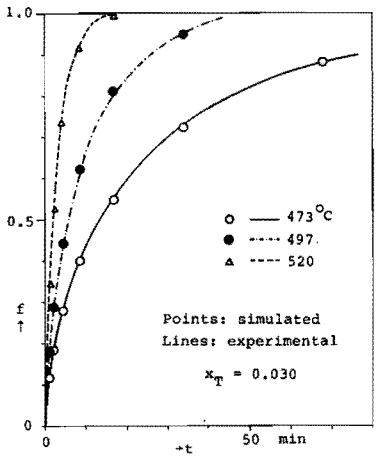

Fig. 5-30

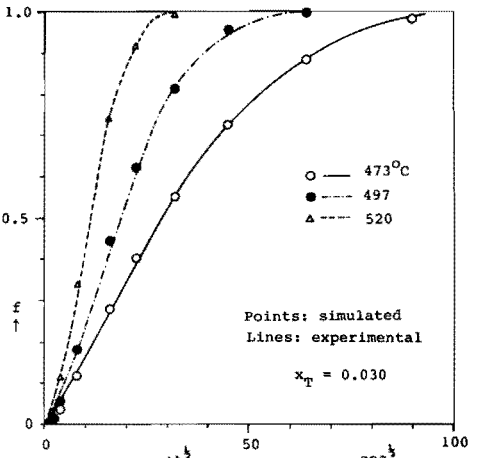

Fig. 5-31

Reduction of bismuth uranate; comparison between simulated and experimental data

However, with a = 200 Å we again obtained for D an energy of activation of 63 kcal.mole^{-1}.

It must be noted that the reduction of Bi_2UO_6 follows the equations (33) and (53) in spite of the fact that the process is actually the sum of a non-selective and a selective reaction, while the ratio between these reactions varies with time. For the reduction rate it appears to be unimportant whether an oxygen atom reacts selectively or not, although in the latter case far less toluene will be converted per atom of oxygen. The question why the selectivity shows such drastic changes in the course of the reaction will be discussed in the next chapter.

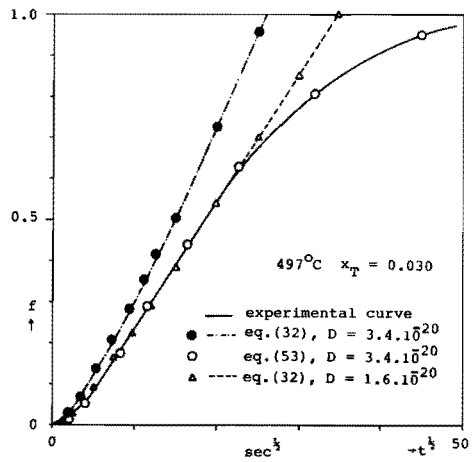

Fig. 5-32 Reduction of bismuth uranate; comparison between experimental and simulated data

Let us now compare the results as obtained with eq. (32), (33) and (53). Except for very low values of f, eq. (32) yields the same curve as eq. (33). In fig. 5-32 one of the experimental curves (solid line) is plotted against $t^{\frac{1}{2}}$, together with the data simulated according to eq. (32) with $D = 3.4 \cdot 10^{-20} m^2.sec^{-1}$ (dots), to eq. (53) with $D = 3.4 \cdot 10^{-20} m^2.sec^{-1}$ (circles), and to eq. (32) with $D = 1.6 \cdot 10^{-20}$ (triangles). Apart from the fact that the use of eq. (33) results in a lower value of D, as was already noted, the agreement between the two models is reasonably good as long as the degree of conversion remains low. Furthermore, the same activation energy is found for D.

With these relations we also determined the diffusion coefficient of the A-site oxygen: (a) from toluene oxidation experiments; toluene mole fraction 0.0030; (b) from benzene oxidation experiments at $\alpha < 5\%$; benzene mole fraction 0.0307. At 470°C, D is $3 \cdot 10^{-22} m^2.sec^{-1}$. The activation energy is 26 kcal. $mole^{-1}$ in both cases. When the activation energy of D was determined from benzene oxidation runs at high α, 63 kcal.$mole^{-1}$ was found, just as in the toluene oxidation experiments. This illustrates that indeed two kinds of lattice oxygen exist, the reactive A-type with low D, and the less reactive but more selective B-type with high D and a high energy of activation for D.

The concept of two types of oxygen has also been brought forward by Grasselli and Suresh (20) for the antimony/uranium oxide catalyst, and by Boreskov et al.(21) for the iron/antimony oxide catalyst. During reduction in a pulse system the latter catalyst behaves similary to bismuth uranate. Boreskov attributes this to the presence of a surface layer of non-selective oxygen. Grasselli found that his catalyst contains 0.65% of selective oxygen, further reduction leading to total combustion of the substrate. He states that one of the four types of oxygen of the unit cell is responsible for the selective oxidation; however, this cannot be brought in agreement with the unit cell he proposes.

Our experiments clearly indicate that the A-oxygen in bismuth uranate is a special kind of lattice oxygen. As with Grasselli, the quantity is too small to correspond to a special position in the unit cell. A possibility is that bismuth and

antimony uranates have so called shear structures (22). This means that the lattice is built up from blocks consisting of a small number of unit cells, regularly divided by shear planes. The oxygen atoms in these planes have a coordination different from that in the blocks and therefore may exhibit different oxidation properties and diffusion coefficients.

Knowing D, we can prove our previous statement (page 77) that the oxygen removed from bismuth uranate in pulse experiments can be replenished during 5-min interval between the pulses. The calculation procedure used was that of Crank (23). Even if the surface had been reduced completely, it would have taken less than 50 seconds to approach again complete equilibrium between bulk and surface.

5.5.4 The selectivity

It was shown in figures 5-1 and 5-14 that the selectivity, i.e. the number of moles of benzene formed per mole of toluene converted, is a function of α. In pulse experiments there is rapid and unselective oxidation at $\alpha < 0.02$, attributed to A-oxygen, followed by a region in which the selectivity is about 70% up to $\alpha = 0.10$. Thereafter the selectivity again declines. Under pulse conditions $\alpha_{bulk} = \alpha_{surface}$, so that evidently the selectivity has a maximum between 2 and 10% of surface reduction. No pulse experiments were carried out at $\alpha > 12\%$. In the flow system the selectivity at the very beginning of the process is higher than that in the pulse system, but it rises more slowly, and attains its maximum only at $\alpha = 0.10$ (fig. 5-14). If we now realize that in the flow reactor the degree of reduction of the bismuth uranate surface is greater than the overall degree of reduction, we see that the maximum selectivity under flow conditions corresponds to a much higher surface α than in the pulse system. The degree of surface conversion as a function of the degree of bulk conversion was calculated according to eq. (54), and the results are shown in fig. 5-33. It follows that $f_{surface}$ differs considerably from f. At high toluene concentrations $f_{surface}$ already has a value of at least 12%,

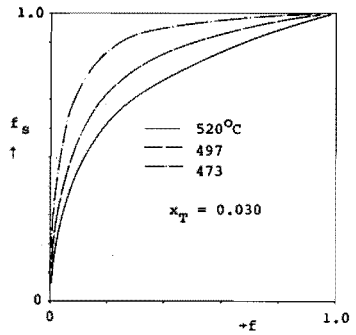

Fig. 5-33 Calculated degree of surface conversion as a function of the degree of bulk conversion

while f is a mere 1%. This proves that the selective region found under pulse conditions, occurs at such very low levels of bulk reduction in the flow system that it will not be found in flow experiments. Instead, the degree of reduction at which the maximum selectivity was found in the flow system corresponds to 28% of surface reduction (fig. 5-34). Apparently the selectivity has another maximum at this value of $f_{surface}$. The high degree of surface reduction under flow conditions also explains why the reaction rates in this system are substantially lower than in the pulse system under identical conditions.

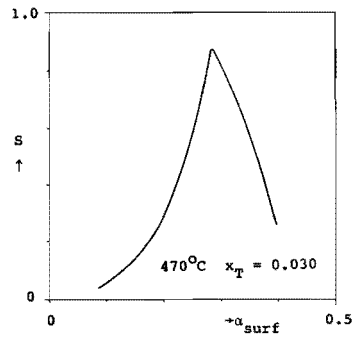

Fig. 5-34 Selectivity as a function of the calculated degree of surface reduction; flow reactor

REFERENCES

1. Von Bogdandy, L., and Engell, H.J., *Die Reduktion des Eisenerze*, Springer-Verlag, Berlin, 1967.
2. Chu, J.C., Kalil, J., and Wetteroth, W.A., *Chem. Eng. Progr.* 49, 141 (1953).
3. Petrovic, L.J., and Thodos, G., *Ind. Eng. Chem. Fund.* 7, 2, 274 (1968).
4. Satterfield, C.N., and Sherwood, T.K., *The Role of Diffusion in Catalysis*, Addison-Wesley, Reading, 1961.
5. Slatterly, J.C., and Bird, R.B., *AICHE J.* 4, 137 (1958).
6. Massoth, F.E., and Scarpiello, D.A., *J. Catal.* 21, 225 (1971).
7. Seth, B.B.L., and Ross, H.U., *Trans. AIME* 233, 180 (1965).
8. Wen, C.Y., *Ind. Eng. Chem.* 60, 9, 34 (1968)
9. Miriyala, V.R.R., and Bowen, J.H., *Can. J. Chem. Eng.* 49, 804 (1971).
10. Calvelo, A., and Cunningham, R.E., *J. Catal.* 17, 1 (1970).
11. Sohn, H.Y., and Szekely, J., *Chem. Eng. Sci.* 27, 763 (1972).
12. Batist, Ph.A., Kapteijns, C.J., Lippens, B.C., and Schuit, G.C.A., *J. Catal.* 7, 33 (1967).
13. Klier, K., and Kučera, E., *J. Phys. Chem. Solids* 27, 1087 (1966).
14. Downie, J., Shelstad, K.A., and Graydon, W.F., *Can. J. Chem. Eng.* 39, 201 (1961).
15. Kumar, R.N., Bhat, G.N., and Kuloor, N.R., *Indian J. Technol.* 3, 83 (1965).
16. Kumar, R.N., Bhat, G.N., and Kuloor, N.R., *Indian Chem. Eng.* 1968, trans. 16.
17. Popova, N.I., and Kabakova, B.V., *Kin. and Catal.* 5, 289 (1964).
18. Reddy, K.A., and Doraiswamy, L.K., *Chem. Eng. Sci.* 24, 1415 (1969).
19. Trimm, D.L., and Irshad, M., *J. Catal.* 18, 142 (1970).
20. Grasselli, R.K., and Suresh, D.D., *J. Catal.* 25, 273 (1972).
21. Boreskov, G.K., Ven'yaminov, S.A., and Pankrat'ev, Yu., *Doklady Chemistry* 196, 55 (1971).
22. Wadsley, A.D., and Andersson, S., *Perspectives in Structural Chemistry*, Vol. III, Wiley, New York, 1970.
23. Crank, J., *The Mathematics of Diffusion*, Oxford University Press, 1956.

CHAPTER 6

THE REACTION MECHANISM

6.1 Introduction

When toluene is brought into contact with bismuth uranate, two reactions take place, viz: the demethylation of toluene to form benzene (the selective reaction), and the complete combustion of toluene (the unselective one). In the preceding chapter we have seen that the selectivity, i.e. the ratio between the rates of these two reactions,depends, among other factors, on the degree of reduction of the oxidant. It appeared that the complete combustion in the initial stages of the reaction is due to the presence of a special kind of lattice oxygen. After removal of these atoms by the hydrocarbon the selective demethylation reaction starts. However, if the degree of reduction at the surface exceeds a certain value, the selectivity declines again, to attain another maximum at a degree of surface reduction of about 30%. This proves that there is no simple relation between the selectivity and the degree of reduction. That the composition of the bismuth uranate and its surface properties also greatly influence the selectivity was already demonstrated in chapter 2. Since our knowledge of the crystallographic properties of bismuth uranate is limited, we shall not try to correlate the selectivity to special surface configurations, but confine ourselves to find possible reaction mechanisms for the two reactions.

For the mechanism of the oxidative demethylation reaction, two routes may be suggested:

a. oxidation of toluene to benzaldehyde, followed by dissociation into benzene and CO (decarbonylation mechanism);
b. oxidation to benzoic acid, either via benzaldehyde or not, followed by dissociation into benzene and CO_2 (decarboxylation mechanism).

Each step of these routes is a plausible reaction. The oxidation of toluene to benzaldehyde occurs over a great number of single or mixed oxides, including bismuth molybdate which is, as we have already seen, in many respects related to bismuth uranate. The reaction is comparable with the oxidation of propylene to acrolein, both substrates having an allyl structure. The oxidation of benzaldehyde to benzoic acid is also well known. Sachtler et al. have demonstrated that this reaction can proceed in absence of oxygen using tin vanadate as oxidant (1). Dissociation of benzaldehyde and benzoic acid can proceed both thermally and catalytically. The thermal decarbonylation of benzaldehyde is slow as compared with our reaction (2) and yields a substantial amount of biphenyl, which is found in our reaction products in traces only. Therefore, the thermal dissociation cannot play an important role in the reaction mechanism. The same applies to the thermal dissociation of benzoic acid.

As to the catalytic decarbonylation of benzaldehyde not much is known. In the early literature the catalytic activity of Pd and Pt is mentioned (3). Both in the thermal and the catalytic reaction CO should be found, which is absent in our reaction products.

The catalytic decarboxylation of benzoic acid can proceed over a great number of metal or metal oxide catalysts. As early as 1914 Sabatier and Mailhe (4) studied this reaction and found that the best yields could be obtained using CdO, ZnO or TiO_2 as catalysts. It is noteworthy that CdO and ZnO are mentioned by Norton and Moss (5) as very suitable catalysts for the oxidative demethylation of alkylaromatics. The decarboxylation with tin vanadate was described by Suvorov and Sembaev (6). The reaction almost certainly involves the formation and subsequent dissociation of a metal benzoate. That pyrolysis of metal benzoates can produce benzene is well known (7). The reaction was studied in more detail for Ni benzoate by Galwey (8).

In order to elucidate whether the demethylation with bismuth uranate proceeds via the decarbonylation or the decarboxylation route, we investigated the interaction between bismuth uranate and benzaldehyde, carbon monoxide and benzoic acid, and also studied the pyrolysis of bismuth and uranium

benzoates.

6.2 The reaction between bismuth uranate and benzaldehyde

The presence of traces of benzaldehyde among our reaction products gave evidence of that benzaldehyde might be an intermediate product. Therefore, the reaction between bismuth uranate and benzaldehyde was investigated both in the pulse and in the continuous flow system, described in chapter 3.

The pulse experiments were carried out with nitrogen/benzaldehyde mixtures containing 1.3 and 17 mole per cent of benzaldehyde and with 0.1, 0.2 and 0.3 g of Bi_2UO_6. In the chromatograms a small peak was present, having a retention time lying between that of benzene and benzaldehyde and not corresponding to the retention time of any simple hydrocarbon which could be expected to be a reaction product. No benzaldehyde peak was detectable, not even after a large number of pulses and at reaction temperatures as low as 400°C. When after some pulses the temperature of the solid was increased, a big and broad signal appeared on the chromatogram, indicating a desorption of hydrocarbon from the surface of the Bi_2UO_6. Evidently, benzaldehyde in some form is strongly adsorbed on bismuth uranate. Desorption of this material either does not occur at all under normal reaction conditions or is so slow that the desorbed benzaldehyde cannot be detected as a peak in the chromatogram. The former explanation is probably incorrect, since the benzaldehyde peak remained absent in the chromatogram even after a number of pulses of benzaldehyde had been given exceeding a complete coverage of the bismuth uranate surface. In the flow reactor the effluent consisted only of CO_2, H_2O, unconverted benzaldehyde and small quantities of benzene. We therefore concluded that the unknown signal present in the chromatograms of the pulse system probably originated from benzene, the long retention time being caused by a strong adsorption of benzaldehyde or a reaction intermediate on the surface. Benzene itself is, as we know from chapter 5, not adsorbed in significant amounts.

The strong adsorption of benzaldehyde and the low rate of formation of benzene from benzaldehyde rule out the possibility

of the oxidative demethylation reaction proceeding with benzaldehyde as an intermediate.

6.3 The reaction between bismuth uranate and carbon monoxide

The fact that CO is absent among our reaction products might be interpreted as another indication against the decarbonylation mechanism. However, the absence of CO can also be caused by a rapid and complete conversion of CO to CO_2 by bismuth uranate. Therefore, we briefly investigated the latter reaction in the flow system. A mixture of 50 vol% CO and 50 vol% N_2 was passed over 1 g of bismuth uranate at 450°C, gas flow 5 $cm^3.min^{-1}$. These conditions were far less favourable for the CO oxidation than was to be expected during the demethylation process. Nevertheless, it appeared that CO was converted quantitatively into CO_2 as long as the degree of reduction of the bismuth uranate did not exceed 40%. Beyond this limit both CO and CO_2 were detectable in the product gas, while the rate of CO oxidation dropped to zero at 60% reduction.

Evidently, the oxidation of CO by Bi_2UO_6 is very fast, hence the absence of CO among the products of the toluene demethylation reaction cannot give evidence of the correctness of one of the proposed mechanisms.

To explore the possibility of using bismuth uranate as a catalyst for the oxidation of CO, for instance in automobile exhaust gases, we also carried out experiments with CO/O_2 mixtures. Results were promising. As an illustration: a mixture of 12 vol% CO, 30 vol% CO_2, 11 vol% O_2 and 44 vol% N_2 passed over 3 g of bismuth uranate at a total gas flow rate of 100 $cm^3.min^{-1}$, was completely oxidized at temperatures above 350°. The reaction started already at 250°. The apparent energy of activation was 17 $kcal.mole^{-1}$. These investigations are to be continued.

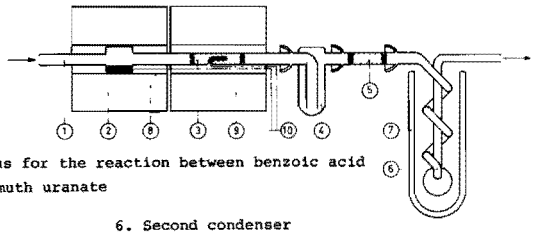

Fig. 6-1 Apparatus for the reaction between benzoic acid and bismuth uranate

1. Quartz tube
2. Molten benzoic acid
3. Bismuth uranate
4. First condenser
5. Magnesium perchlorate tube
6. Second condenser
7. Dewar vessel
8. First furnace
9. Second furnace
10. Thermocouples

6.4 The reaction between bismuth uranate and benzoic acid

The interaction between benzoic acid and bismuth uranate was studied in the apparatus shown in fig. 6-1. Owing to the high melting point of the benzoic acid (122°C) and the viscosity of the melt, vaporizers of the type used for the preparation of nitrogen/toluene mixtures were difficult to use. Therefore, we simple passed dried, oxygen-free nitrogen over molten benzoic acid to obtain a gas mixture, not completely saturated with benzoic acid, but having a composition sufficiently constant for our purposes. With a nitrogen flow of 25 $cm^3.min^{-1}$, the benzoic acid mole fraction appeared to be 0.017. The reactor tube was identical with that of the flow system and was filled with 2.3 g of Bi_2UO_6. The reactor effluents first passed a small, air-cooled condenser, in which non-converted benzoic acid and high-boiling reaction products deposited. Then the gas was passed through a tube filled with magnesium perchlorate in which the water produced was absorbed. It was established that no hydrocarbons were condensed in this tube. The remaining components were collected in a second condenser, cooled with a dry ice/acetone mixture. The condensate in this cold trap was dissolved in a known amount of carbon tetrachloride and analysed by gas chromatography. Benzene was the only reaction product detectable. The quantity of benzene followed from the ratio of the peak areas of carbon tetrachloride and benzene. The amount of water followed from the increase in weight of magnesium perchlorate tube. The reaction conditions were such that the benzoic acid in the feed gas was completely converted, according to the equations:

$$C_7H_6O_2 \rightarrow C_6H_6 + CO_2$$

$$x\ C_7H_6O_2 + 15\ Bi_2UO_6 \rightarrow 7x\ CO_2 + 3x\ H_2O + 15\ Bi_2UO_{6-x}$$

During an experiment, the amounts of benzene and water were determined every 15 minutes. During such a period, approx. 10% of the oxygen atoms of the bismuth uranate had been removed. From the results, the amount of converted benzoic acid, the degree of reduction of the bismuth uranate, and the selectivity were calculated. In fig. 6-2 the selectivity is plotted as a function of the degree of reduction for three temperatures. It must be emphasized that the selectivities were obtained over ranges covering degrees of reduction of about 10%. For that reason, and because of the long bed of bismuth uranate used, the selectivity curve may have been spread and may not be comparable with that obtained in the flow system during toluene oxidation experiments.

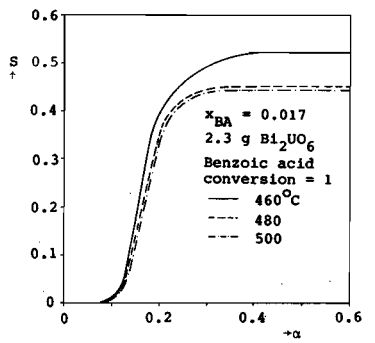

Fig. 6-2 Selectivity in benzene during the reaction between bismuth uranate and benzoic acid as a function of the degree of reduction

It appears that benzoic acid can be converted into benzene with a selectivity of the same order of magnitude as that observed during the toluene demethylation process. Moreover, the rate of the reaction is high, even at high degrees of reduction of the oxidant.

6.5 Preparation of bismuth and uranium benzoates

An ammonium benzoate solution was prepared by dissolving benzoic acid in ammonia. This solution was added to a solution of bismuth nitrate in dilute HNO_3. The precipitate was washed

with water, alcohol and ether and dried, to yield a white and amorphous substance. It was identified as bismuthyl benzoate, $BiO(C_7H_5O_2)\cdot 4.4H_2O$. Various attempts to obtain bismuth benzoate, $Bi(C_7H_5O_2)_3$, were unsuccessful, which is not surprising since it is known that bismuth salts rapidly hydrolize into the corresponding bismuthyl salts. A similar ammonium benzoate solution was added to a solution of uranyl acetate in hot water. A yellow precipitate formed, which was washed with water and dried. The product consisted of bright yellow needles, and proved to be the uranyl benzoate, $UO_2(C_7H_5O_2)\cdot 4.4H_2O$.

6.6 Pyrolysis of bismuth and uranium benzoates

Both bismuth benzoate and uranium benzoate were subjected to pyrolysis, carried out with a few grams of material under nitrogen in a small tubular reactor, directly connected to an ice-cooled condenser. The temperature was increased at the rate of 10°C per min. Both samples behaved almost identically. First they lost water at 100-160°C. At 320° white clouds started to evade, followed by a clear liquid at 370-400°. Above 400° a yellow solid condensed. The contents of the condenser were dissolved in ether and analysed by gas chromatography. Benzene proved to be present in traces only. After that, the solution was thoroughly shaken with an ammonium bicarbonate solution. The layers were separated and evaporated. By far the greater part of material was obtained from the layer water. This product was colourless and was identified as ammonium benzoate. That from the ether layer was yellow and the IR and PMR spectra showed the presence of aromatic ring systems. These results prove that by heating the benzoates slowly to 400°, benzene is obtained in a small yield only, the main product being benzoic acid. At higher temperatures tar-like substances containing aromatic rings are also formed.

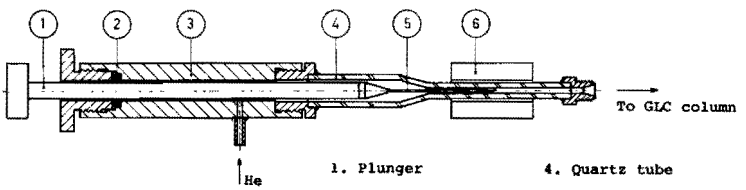

1. Plunger
2. O-ring sealing
3. Housing
4. Quartz tube
5. Hollow needle
6. Furnace

Fig. 6-3 Pyrolysis apparatus

Rapid pyrolysis of the compounds was carried out in apparatus depicted in fig. 6-3. Carrier gas (helium) was passed through a quartz tube, i.d. 2 mm, heated to 450^{o} by a furnace and enter the column of a gas chromatograph (stationary phase DC 550, 180^{o}). By means of a hollow needle a few µg of the sample were introduced into the tube without interrupting the gas flow. Because of the low heat capacity of the needle and the sample, the latter almost instantly took the desired temperature. The products formed were separated on the column and detected with a flame ionisation detector. Peaks were identified by comparing the retention times with those of the pure substances.

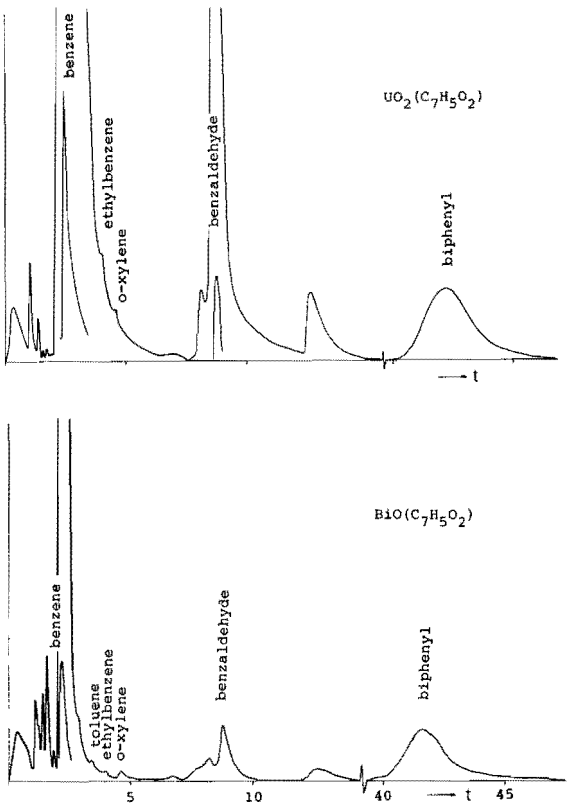

Fig. 6-4 Pyrograms of bismuth and uranium benzoates; 450^{o}C

Fig. 6-4 gives the chromatograms obtained by pyrolysis of bismuth and uranium benzoate. It is evident that considerable amounts of benzene were formed, together with benzaldehyde, biphenyl, and traces of toluene, xylene and various volatile cracking products. The quantitative reproducibility of these experiments was rather poor. Therefore, we confine ourselves to giving the ratio of the peak areas of a few compounds to the total peak area of all components detected in the experiments of fig. 6-4:

	benzene	benzaldehyde	biphenyl
bismuth benzoate	0.66	0.15	0.17
uranium benzoate	0.73	0.19	0.06

To account for the differences in product distribution between the experiments with slow temperature increase in the tubular reactor and with very rapid temperature increase by means of the hollow needle technique we can give two explanations. The first is that the reaction mechanism at low temperatures differs from that at 450°. The second is that during the slow pyrolysis the crystal water of the substance is liberated before the actual pyrolysis reaction starts, so that the latter reaction is carried out in absence of water. At 450°, on the other hand, the pyrolysis and the dehydration take place at the same time, an excess of water being evolved which can play a role in the reaction.

To check whether the second hypothesis could be correct, a sample of uranyl benzoate was subjected to rapid pyrolysis after pre-heating at 160° for 30 minutes. Indeed, we observed a considerable decrease in the benzene peak area, indicating that the presence of water strongly enhances the formation of benzene. From the observation that during the pyrolysis of bismuth and uranium benzoates the metal ion is reduced, viz. from hexavalent uranium to UO_2 and from trivalent bismuth to bismuth metal, it can be concluded that during pyrolysis the benzoate is partly oxidized under formation of CO_2 and H_2O. However, this amount of water is apparently insufficient for a high benzene production.

6.7 Discussion

The results obtained so far indicate that the demethylation reaction may proceed according to the decarboxylation mechanism:

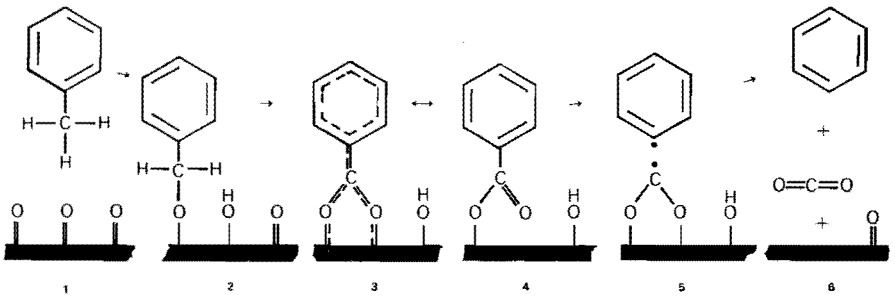

First, toluene is oxidized to benzoic acid. This reaction can be visualized as a sequence of hydrogen abstraction steps, followed by formation of carbon-oxygen bonds. The abstracted hydrogen atoms form hydroxyl groups at the bismuth uranate surface and eventually dissociate as water molecules. The benzoate intermediate may have the structure (3) as was found by Sachtler for the oxidation of benzaldehyde to benzoic acid over tin vanadate (1). The next step is the breaking of the bond between the aromatic nucleus and the side chain of the benzoate under the formation of a phenyl radical. This reaction is comparable to the pyrolysis of metal benzoates. The phenyl radical abstracts a hydrogen from one of the adjoining hydroxyl groups and forms benzene. Meanwhile, the remaining carboxyl group dissociates from the surface as CO_2.

If no hydroxyl groups, from which hydrogen atoms can be abstracted, are present, the phenyl radicals will recombine to form biphenyl or higher-boiling compounds. Since the OH groups are in equilibrium with water vapour, the presence of the

latter in the reaction gas will greatly enhance the benzene formation. This was demonstrated by Suvorov and Sembaev (6) during a study of the decarboxylation of benzoic acid over tin vanadate. It is also in agreement with our findings that with pyrolysis of uranyl benzoate the benzene yield is much lower with a sample preheated at 160°C to remove adsorbed water than with a sample containing crystal water. The absence of any influence of the addition of water to the feed gas in our reaction system is explained by the fact that much water is already produced during the reaction. If the selectivity is 75%, 1.75 moles of water are formed per mole of toluene converted, which value rises to 2.5 at selectivity 50%.

It is rather surprising that benzaldehyde shows a different behaviour when contacted with bismuth uranate. The adsorption of benzaldehyde would probably lead to one of the structures (3) or (4). A possibility is that as soon as free gaseous benzaldehyde is present, it is adsorbed on another type of sites, on which a different reaction mechanism is operative. A feature of the selective reaction described so far is that it only occurs on a reduced bismuth uranate surface (see section 5.1.1). Since the reduction is coupled with the formation of bismuth metal, it is not impossible that metallic bismuth plays a role in the demethylation mechanism.

The origin of the complete combustion of toluene is more difficult to establish. This reaction is especially favoured by the presence of A-oxygen, identified by a high reaction rate and low rate of diffusion through the lattice. Assuming that the metal oxygen bond strength of this A-oxygen is smaller than that of the B-site oxygen, its oxidation behaviour can be brought in agreement with the concept prevailing among a number of authors (1, 9) that the total combustion during catalytic oxidation of hydrocarbons is related to a low metal-oxygen bond strength in the catalyst. Since benzene is also converted by A-oxygen, it appears that a direct attack on the aromatic nucleus takes place. Benzene, i.e. the aromatic nucleus, is almost stable under pulse conditions after removal of the A-oxygen. Even then, however, the selectivity of the oxidation of toluene is never higher than approx. 70%, indicating that there is another non-selective reaction, acting on the side chain of the molecule.

The energies of activation of the demethylation and combustion processes are almost equal. This suggests that a common intermediate exists, the formation of which is the rate-determining step. The intermediate could very well be the benzoate group, since it has been demonstrated that the dissociation of this structure takes place with a selectivity comparable to that of the toluene oxidation.

REFERENCES

1. Sachtler, W.M.H., Dorgelo, G.J.H., Fahrenfort, J., and Voorhoeve, R.J.H., *Rec. Trav. Chim.* 89, 460 (1970).
2. Hurd, C.D., and Bennett, C.W., *J. A. C. S.* 51, 1197 (1929).
3. Peytral, E., *Bull.* 4 29, 44 (1921).
4. Sabatier, P., and Mailhe, A., *C. R.* 159 (3), 28 (1914).
5. Norton, C.J., and Moss, T.E., *U.S. Pat.* 3,175,016 (1965).
6. Suvorov, B.V., and Sembaev, D.K., *IVth International Congress on Catalysis*, Moscow 1968; Umarova, R.U., Sembaev, D.K., and Suvorov, B.V., *Izv. Akad. Nauk Kaz. SSR*, Ser. Khim. 19, 30 (1969) and: *C. A.* 72, 3120 (1970).
7. *Beilsteins Handbuch der Organischen Chemie*, Syst. Nr. 897, Springer-Verlag, Berlin 1970.
8. Galwey,A.K., *J. Catal.* 4, 34 (1965).
9. Boreskov, G.K., Popovsky, V.V., Sazonov, V.A., *IVth International Congress on Catalysis*, p. 580, Moscow (1968).

CHAPTER 7

OTHER CATALYSTS FOR THE OXIDATION OF TOLUENE

7.1 Mixed metal oxides

It has already been mentioned in chapter 1 of this thesis that in the literature a great number of catalyst systems is described, mostly of an oxidic nature, for the oxidation of toluene. Some of the best catalysts were summarized in table 1-1. A comprehensive review on this subject is given by Dixon (1). More recently a survey of the activity of 22 single metal oxides was given by Germain (2). We screened several binary oxide catalysts in the pulse system, and used a nitrogen/toluene mixture as the feed gas. This is, of course, a rather unusual procedure. On the other hand, if under these conditions the selectivity is low, it will most probably not be better if gaseous oxygen is present, nor is an improvement to be expected in a flow system. Therefore, a provisional indication of the suitability of a given catalyst can be obtained. The method of preparation of the catalysts is given in table 7-1. The colour and, in some cases, the surface area have also been listed.

Each substance was tested under several conditions. The reaction temperature was varied between 400 and 470^{o}C, the toluene mole fraction between 0.01 and 0.10. Approximately 1 g of catalyst was used. The best results are summarized in table 7-2. Omitted from this table have been bismuth oxide, uranium oxide and the various bismuth uranates, already described in full detail; promoted bismuth uranates and the bismuth phosphate system will be discussed separately in this chapter.

It is difficult to find any regularity in these results. Some catalysts, known to be selective for the oxidation of propylene or butene, e.g. bismuth molybdate, are selective for the oxidation of toluene as well, but others, such as uranium antimonate, do not give satisfactory results. Both cadmium oxide and some uranates act selectively, but cadmium uranate is the least selective of all compounds tested. This illustrates

the difficulty of predicting the activity of a catalyst on the basis of composition only. The best way to select a catalyst for a given reaction still seems to be the method of trial and error.

7.2 Promoted Bismuth Uranates

The addition of a few per cent of a substance to a catalyst can sometimes have a great effect on its activity. If the new catalyst gives more satisfactory results than the original one, such a substance is called a promotor. Many industrial catalysts contain such promotors. A commercial vanadium pentoxide catalyst is usually promoted with potassium sulfate; the selectivity of bismuth molybdate can be enhanced by adding iron (3). In a similar way we attempted to improve the oxidation properties of bismuth uranate by adding small quantities of the elements P, Sb, Sn, Fe and Li.

Lithium and phosphor promoted bismuth uranates were prepared by impregnating partly reduced samples with dilute solutions of lithium hydroxide and ammonium phosphate, respectively. The treated samples were calcined for 1 hour at 500°.

$Bi_{1.8}Sb_{0.2}UO_6$ was prepared in much the same way as bismuth uranate. $Sb(OH)_3$ was precipitated from an $SbCl_3$ solution by ammonia; the washed precipitate was boiled together with $Bi(OH)_3$ and $UO_2(OH)_2$. The product was filtered off, dried and calcined. The surface area was 16.8 $m^2.g^{-1}$ (BET-method). $Bi_{1.8}Sn_{0.2}UO_{5.9}$ (22.5 $m^2.g^{-1}$) was prepared similarly; $Sn(OH)_2$ was prepared from an $SnCl_2$ solution. $Bi_{1.8}Fe_{0.2}UO_{5.9}$ (9.6 $m^2.g^{-1}$) was prepared with $Fe(OH)_2$ precipitated from $FeCl_2$. Finally, $Bi_2U_{0.5}Mo_{0.5}O_6$ was prepared by boiling $Bi(OH)_3$, $UO_2(OH)_2$ and H_2MoO_4 together. Colours were equal to those of pure bismuth uranate.

Activities were tested in the pulse system as described before. The activity of the lithium and phosphor promoted bismuth uranates was substantially lower than that of the pure Bi_2UO_6. The maximum selectivity and corresponding conversion of the other samples are given in table 7-3.

TABLE 7-1 PREPARATION AND PROPERTIES OF THE CATALYSTS *

Catalyst	Preparation	Colour	Surface Area $m^2.g^{-1}$	Ref.
Cadmium oxide	Obtained commercially (BDH). Calcined 1 hour at 700°C.	Reddish-brown		
Cadmium uranate Cd/U=1	By boiling freshly precipitated cadmium hydroxide and uranyl hydroxide in water. Calcined 1½ hours at 500°.	Orange-brown	5	
Bismuth molybdate Bi/Mo=2	By boiling freshly precipitated bismuth hydroxide and molybdic acid in water. Calcined 1 hour at 550°.	Light yellow	4	(7)
Bismuth tellurate Bi/Te=2	By evaporating a mixture of bismuth hydroxide, telluric acid and ammonia. Calcined 1 hour at 700°.	Light yellow		
Bismuth zincate Bi/Zn=1	By boiling freshly precipitated bismuth hydroxide and zinc hydroxide in water. Calcined 2 hours at 500°.	Light yellow		
Bismuth chromate Bi/Cr=2	By evaporating a mixture of bismuth hydroxide, chromic acid and ammonia. Calcined 1 hour at 400°.	Orange		
Bismuth stannate Bi/Sn=2	By boiling freshly precipitated bismuth hydroxide and stannic hydroxide in water. Calcined 2 hours at 500°.	Light yellow		(14)
Bismuth tungstate Bi/W=2	By boiling basic bismuth nitrate and tungstic acid in water. Calcined 1 hour at 500°.	Light yellow		(15)
Iron molybdate Bi/Fe=2/3	From an iron nitrate solution by precipitation with ammonium molybdate. Calcined 3 hours at 520°.	Greyish green	6	(3)
Iron uranate Fe/U=2/3	By boiling freshly precipitated iron hydroxide and uranyl hydroxide in water. Calcined 2 hours at 500°.	Dark brown		
Iron antimonate Fe/Sb=1	From a solution of antimony pentachloride and iron trichloride by coprecipitation with ammonia. Calcined 8 hours at 700°.	Brownish black	11	(8)

TABLE 7-1 (continued)

Catalyst	Preparation	Colour	Surface Area $m^2.g^{-1}$	Ref
Iron tellurate	By evaporating a mixture of iron trinitrate, telluric acid and ammonia.	Olive		
Chromium molybdate Cr/Mo=2/3	From a chromium trinitrate solution by precipitation with ammonium molybdate.	Green		
Tin antimonate Sn/Sb=1	From a solution of stannic chloride and antimony pentachloride by coprecipitation with ammonia. Calcined 1 hour at 500°.	Greyish green	42	(9)
Tin uranate Sn/U=1	By boiling freshly precipitated, stannic hydroxide and uranyl hydroxide. Calcined 1 hour at 500°.	Greyish green	10	
Uranium antimonate on silica	Commercial catalyst	Pink		(10)
Uranium antimonate U/Sb=1	By boiling freshly precipitated uranium hydroxide and antimony hydroxide in water. Calcined 8 hours at 720°.	Greyish violet		(11)
Uranium molybdate U/Mo=1	By boiling freshly precipitated uranyl hydroxide and molybdate acid in water. Calcined 3 hours at 520°.	Yellow		
Uranium molybdate U/Mo=1/2	Ditto. Calcined 1 hour at 550°.	Yellow		
Uranium tellurate U/Te=1	By evaporating a mixture of uranyl acetate, telluric acid and ammonia. Calcined 1 hour at 480°.	Yellowish orange		
Uranium tellurium molybdate U/Te/Mo=3/1/4	By evaporating a mixture of uranyl acetate, telluric acid, molybdic acid and ammonia. Calcined 1½ hours at 500°.	Light yellow		
Cerium tellurate Ce/Te=2/3	By evaporating a mixture of cerium trinitrate, telluric acid and ammonia. Calcined 1 hour at 480°.	Yellowish brown		
Cerium tellurium molybdate Ce/Te/Mo=1/1/1	By evaporating a mixture of cerium trinitrate, telluric acid, molybdic acid and ammonia. Calcined 1½ hours at 450°.	Yellowish brown		(12)

TABLE 7-1 (continued)

Catalyst	Preparation	Colour	Surface Area $m^2.g^{-1}$	Ref
Copper tellurate Cu/Te=1	By evaporating a mixture of cuprous acetate, telluric acid and ammonia. Calcined 1½ hours at 550°.	Yellowish green		
Copper uranate Cu/U=1	By boiling freshly precipitated cuprous hydroxide and uranyl hydroxide in water. Calcined 2 hours at 500°.	Dark brown	5	
Copper tungstate Cu/W=1	By evaporating a mixture of ammonium tungstate, cuprous nitrate and ammonia. Calcined 2 hours at 500°.	Green		
Zinc chromium ferrite Zn/Cr/Fe=1/1/1	By boiling freshly precipitated zinc hydroxide, chromium hydroxide and iron hydroxide in water. Calcined 1½ hours at 500°.	Black		(13)

* Most of these catalysts were kindly provided by Mr.Ph.A.Batist

TABLE 7-2 ACTIVITY OF A NUMBER OF CATALYST SYSTEMS FOR THE OXIDATION OF TOLUENE

CATALYST	YIELD		
	CO_2	Benzene	Benzaldehyde
Cadmium oxide	+	++	-
Cadmium uranate	++	-	-
Bismuth molybdate	+	+	+
Bismuth tellurate	-	-	-
Bismuth zincate	+	+	-
Bismuth chromate	++	.	-
Bismuth stannate	+	+	-
Bismuth tungstate	++	-	-
Iron molybdate	++	.	-
Iron uranate	++	-	-
Iron antimonate	+	+	.
Iron tellurate	++	-	-
Chromium molybdate	++	-	-
Tin antimonate	++	.	-
Tin uranate	++	-	-
Uranium antimonate on silica	++	.	-
Uranium antimonate	++	-	-
Uranium molybdate 1/1	+	.	+
Ditto, 1/2	++	.	.
Uranium tellurate	+	-	+
Uranium tellurium molybdate	++	-	-
Cerium tellurate	++	-	-
Cerium tellurium molybdate	++	-	++
Copper tellurate	++	-	.
Copper uranate	++	+	.
Copper tungstate	++	.	-
Zinc chromium ferrite	++	-	-

++: high
+: fair
.: low
-: nil

Test conditions: pulse reactor, 400-470°C, toluene/nitrogen mixture, toluene mole fraction 0.01-0.10, 0.5-1.0 g of catalyst.

TABLE 7-3 ACTIVITY OF PROMOTED BISMUTH URANATES

	Temperature	Maximum Selectivity	Conversion
Bi_2UO_6	475 °C	70 %	85 %
$Bi_{1.8}Sb_{0.2}UO_6$	446	30	40
	487	35	47
$Bi_{1.8}Sn_{0.2}UO_{5.9}$	430	65	85
	470	41	90
$Bi_{1.8}Fe_{0.2}UO_{5.9}$	440	31	58
	475	25	85
$Bi_2U_{0.5}Mo_{0.5}O_6$	475	--	10

Evidently, only the addition of tin has a positive effect on the oxidation properties of bismuth uranate. The same conversion can be attained at a temperature 45° lower than that of the non-promoted compound. The selectivity, however, is not increased.

7.3 Bismuth phosphates

It is known that bismuth phosphates can act as selective catalysts for the oxidation of hydrocarbons. A patent of Voge and Adams (4) described a bismuth phosphate catalyst for the oxidation of butene to butadiene, whilst recently Sakamoto (5) and Seiyama (6) reported on the possibility of oxidizing propylene to hexadiene and benzene over the same material. Exploratory studies in our pulse apparatus showed that bismuth phosphate can also act as a toluene demethylation catalyst. Therefore we decided to examine the bismuth phosphates in more detail. Bismuth phosphates with Bi/P=½, 1, 3/2, 5/2 and 3 were prepared according to (5). Bismuth nitrate or basic nitrate was dissolved in dilute HNO_3. By adding a solution of diammonium hydrogenphosphate a precipitate formed, which was filtered off, dried at 150° and calcined for 1 hour at 500°. White, amorphous solids were obtained. Specific surface areas were 11.3, 11.8, 8.3, 9.0, 9.6 and 9.0 $m^2.g^{-1}$, respectively. A sample of

$Bi_4(P_2O_7)_3$ was prepared by mixing solutions of $Bi(NO_3)_3$ and $Na_4P_2O_7$. The precipitate was dried under diminished pressure at room temperature to prevent hydrolysis, and calcined for 1 hour at 500°.

The catalysts were first tested in the pulse system in the absence of air. $Bi_4(P_2O_7)_3$ shows no selectivity at all, and will no longer be discussed. With the other samples substantial amounts of benzene and traces of benzaldehyde are produced, but after a few pulses the activity falls steadily. The solids turn grey, but regain their original colour by reoxidation. Probably the bismuth phosphates are reduced and metallic bismuth forms. When sufficient oxygen is added to the feed gas, the activity remains constant. The outcome of a series of experiments carried out with 0.5 g of catalyst and a feed gas consisting of 88.2% N_2, 10.9% O_2 and 0.9% toluene is given in figure 7-1.

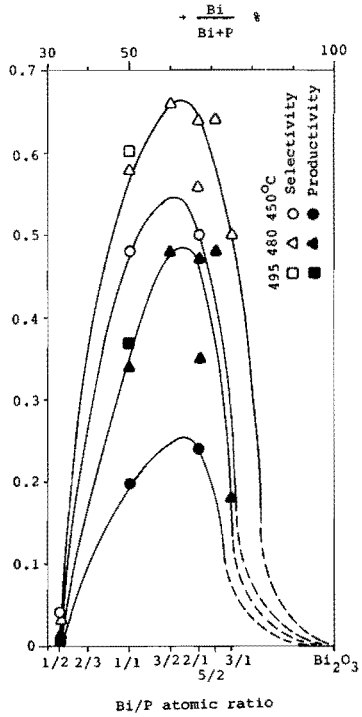

Fig. 7-1 Selectivity and productivity of the toluene demethylation reaction over bismuth phosphate catalysts; 0.5 g catalyst, feed gas 88.2% N_2, 10.9% O_2, 0.9% toluene; pulse reactor

Both the selectivity and the productivity have a pronounced maximum when the Bi/P ratio is about 2. It is reported by Sakamoto that the same catalyst is also the most selective Bi/P compound for the oxidation of propylene to hexadiene and benzene. An X-ray analysis of this catalyst revealed (6) that the material actually consists of a mixture of α-,β-,and γ-$BiPO_4$, $2Bi_2O_3.P_2O_5$, $3Bi_2O_3.P_2O_5$ and γ-Bi_2O_3. Which of these compounds is the active component has not yet ascertained. The catalyst with Bi/P=2 was also tested in the continuous flow apparatus described in chapter 3. As a feed gas we used an air/toluene mixture with such a ratio that there was always gaseous oxygen present in the effluent. The results of four runs under steady state conditions are given in table 7-4.

TABLE 7-4 ACTIVITY OF BISMUTH PHOSPHATE Bi/P=2

Run number	Temperature °C	Gas flow $cm^3.min^{-1}$	Composition %			Toluene Conversion %	Benzene Productivity %	Benzene Selectivity %
			Toluene	N_2	O_2			
1	480	6.0	12.1	70.3	17.6	30	7.5	25
2	450	4.0	7.9	73.7	18.4	40	8	20
3	480	4.0	7.9	73.7	18.4	46	11	24
4	480	4.2	3.9	76.8	19.3	80	16	20

Comparison of runs 2 and 3 shows that an increase in the reaction temperature has only a slight effect on the conversion, i.e. the apparent energy of activation is low. From experiments 3 and 4 it can be seen that the conversion rises sharply with decreasing toluene concentration, indicating a reaction order in toluene well below 1.

In all experiments the selectivities are low. The values obtained in the pulse system could by no means be reproduced under continuous flow conditions. However, the results obtained so far should justify a further investigation of the bismuth phosphate system.

REFERENCES

1. Dixon, J.K., and Longfield, J.E., *Catalysis*, vol.7, Emmett, Ed.Reinhold, 1960.
2. Germain, J.E., and Laugier, R., *Bull.* 1972, 541.
3. Batist, Ph.A., van de Moesdijk, C.G.M., Matsuura, I., and Schuit, G.C.A., *J.Catal.* 20, 40 (1971).
4. Voge, H.H., and Adams, C.R., *U.S.P.* 2,991,321 (1959); *C.A.* 56, 6706 (1962).
5. Sakamoto, T., Egashira, M., and Seiyama, T., *J.Catal.* 16, 407 (1970).
6. Seiyama, T., Egashira, M., Sakamoto, T., and Aso, I., *J.Catal.* 24, 76 (1972).
7. Batist, Ph.A., Bouwens, J.F.H., and Schuit, G.C.A., *J. Catal.* 25, 1 (1972).
8. Boreskov, G.K., Ven'yaminov, S.A., Dzis'ko, V.A., Tarasova, D.V., Dindoin, V.M., Sazonova, N.N., Olen'kova, I.P., and Kefeli, L.M., *Kin.and Catal.* 10, 1109 (1969).
9. Trimm, D.L., and Gabbay, D.S., *Trans.Farad.Soc.* 67, 2782 (1971).
10. Callahan, J.L., and Gertisser, B., *U.S.P.* 3,198,750 (1965).
11. Simons, Th.G.J., Houtman, P.N., and Schuit, G.C.A., *J. Catal.* 23, 1 (1971).
12. Montecatini Edison S.p.A., *Dutch Pat.* 6,611,998 (1967).
13. Kehl, W.L., and Rennard, R.J., *U.S.P.* 3,450,788 (1969). Rennard, R.J., and Kehl, W.L., *J.Catal.* 21, 282 (1971).
14. Ohdan, K., Ogawa, T., Umemura, S., Yamada, K., *Kogya Kagaku Zasshi* 73 842 (1970); *C.A.* 73 44803 (1970).
15. Ohdan, K., Umemura, S., Yamada, K., *Kogyo Kagaku Zasshi* 73 441 (1970); *C.A.* 73 13885 (1970).

SUMMARY

Toluene, brought in contact with various bismuth uranates in a stream of an inert gas at 400-500°C, is oxidized to benzene, CO_2 and H_2O. The highest benzene yields are obtained with the compound Bi_2UO_6 with high specific surface area. During the reaction bismuth uranate can lose about 67% of its oxygen atoms under formation of metallic bismuth and UO_2. The original activity is completely restored by oxidation with molecular oxygen. This opens the possibility of demethylating toluene by passing air and toluene over bismuth uranate alternatingly.
The kinetics of the reduction of bismuth uranate with toluene were investigated in micro-pulse and micro-flow reactors and in a thermobalance. The kinetics of the surface reaction were determined in the pulse system. The reaction proceeds according to a first-order parallel scheme with an activation energy of 30 kcal.mole^{-1}. In the flow system and in the thermobalance the rate of oxygen diffusion through the lattice also plays a role. The kinetics could be described by an equation that comprised both the chemical reaction and the diffusion. Agreement with the experimental data is good. It appears that bismuth uranate contains two different types of lattice oxygen, a non-selective one with diffusion coefficient $D = 3.10^{-22}$ m^2.sec^{-1} and a diffusion activation energy $E = 26$ kcal.mole^{-1}, and a more selective one with $D = 3.10^{-20}$ and $E = 63$ (at 470°C).
The reaction of bismuth uranate with CO, benzaldehyde and benzoic acid as well as the pyrolysis of bismuthyl and uranyl benzoates were studied. From the results we concluded that the selective reaction probably proceeds via a benzoate-like intermediate.
The activity of a great number of other binary oxides in toluene oxidation was investigated. Promising results were obtained with the bismuth phosphate system.

SAMENVATTING

Wanneer tolueen in een stroom inert gas over bismuth uranaat wordt geleid, wordt het geoxideerd tot benzeen, CO_2 en H_2O. De hoogste benzeenopbrengsten verkrijgt men met de verbinding Bi_2UO_6 met een hoog specifiek oppervlak. Bij de reactie kan bismuth uranaat ongeveer 67% van zijn zuurstofatomen verliezen, waarbij metallisch bismuth en UO_2 ontstaan. De oorspronkelijke activiteit kan volledig worden hersteld door oxidatie met moleculaire zuurstof. Dit maakt het mogelijk tolueen te demethyleren door afwisselend lucht en tolueen over bismuth uranaat te leiden.

De kinetiek van de reactie van bismuth uranaat met tolueen werd onderzocht in micro-puls- en micro-flowreactoren en in een thermobalans. De kinetiek van de oppervlaktereactie werd bepaald in de pulsreactor. De reactie verloopt volgens een eerste-orde parallel schema met een activeringsenergie van 30 $kcal.mol^{-1}$. In de flowreactor en de thermobalans speelt de diffusiesnelheid van zuurstof door het rooster naar het oppervlak ook een rol. De kinetiek kan worden beschreven met een vergelijking die zowel de chemische reactie als de diffusie omvat. De overeenkomst met de experimentele resultaten is goed. Het blijkt dat bismuth uranaat twee soorten roosterzuurstof bevat: een niet-selectieve met een diffusiecoëfficient $D = 3.10^{-22}$ $m^2.sec^{-1}$ en een diffusie-activeringsenergie $E = 26$ $kcal.mole^{-1}$, en een meer selectieve met $D = 3.10^{-20}$ en $E = 63$ (bij 470°C).

We bestudeerden voorts de reactie van bismuth uranaat met CO, benzaldehyde en benzoëzuur en de pyrolyse van bismuthyl en uranyl benzoaat. Uit de resultaten kon worden afgeleid dat de selectieve reactie vermoedelijk verloopt via een benzoaat-achtig intermediair.

De activiteit van een groot aantal andere binaire oxiden voor de oxidatie van tolueen werd onderzocht. De resultaten verkregen met bismuth fosfaten waren veelbelovend.

LIST OF SYMBOLS

Latin symbols		units*
a	crystallite radius	Å
A	constant	
A_x	peak area of component x	
B	constant	
(B)	benzene concentration	$mole.m^{-3}$
c, c(r,t)	oxygen concentration in solid	$atoms.m^{-3}$
C_o, C_s	substrate concentration	$mole.m^{-3}$
C	constant, conversion	
d	surface layer thickness	Å
D	diffusion coefficient of lattice oxygen	$m^2.sec^{-1}$
$D_{1,2}$	free gas diffusion coefficient	$cm^2.sec^{-1}$
D_{eff}	effective gas diffusion coefficient	$cm^2.sec^{-1}$
D_{knud}	Knudsen diffusion coefficient	$cm^2.sec^{-1}$
E	energy of activation	$Kcal.mole^{-1}$
f	degree of conversion	
f_s	degree of surface reduction	
f_x	response factor of component x	
k, k', k_v	reaction rate constant	$m^3.mol^{-1}.sec^{-1}$, sec^{-1}
k_{gm}	mass transfer coefficient	$sec.m^{-1}$
M	molecular weight	
n	reaction order, number of moles	
N	number of pulses	
(O)	oxygen concentration	$atoms.m^{-3}$
p_g	partial pressure in the gas bulk	$N.m^{-2}$
p_s	partial pressure at the surface	$N.m^{-2}$
p	pressure	$N.m^{-2}$
r	distance to centre of particle	Å
r_c	crystallite radius	Å
r_o	particle radius	cm
r_p	pore radius	Å
R	gas constant	$Kcal.mole^{-1}.K^{-1}$
S	specific surface area	$m^2.g^{-1}$
S	selectivity	

t	time	sec, min
T	temperature	^{o}C, K
V_c	catalyst volume	cm^3
X_x	mole fraction of component x	

Greek symbols

α	degree of reduction	
α_∞	degree of reduction at infinite time	
η	effectiveness factor	
λ	jump distance	cm
ρ	density	$g.cm^{-3}$
τ	time required for complete conversion	sec
τ_p	tortuosity factor	
ϕ_m	mass flux	$kg.m^{-2}.sec^{-1}$
ϕ_x	mole flux of component x	$mole.m^{-2}.sec^{-1}$
ϕ_{Th}	Thiele modulus	

* unless stated otherwise

I

Tolueen kan oxidatief in benzeen worden omgezet door afwisselend tolueen en zuurstof over bismuth uranaat te leiden.

Dit proefschrift

II

Voor het meten van CO- en CO_2-concentraties in gasmengsels biedt het gebruik van de Maihak MONO-analysator dikwijls voordelen boven fotometrische of gaschromatografische methoden.

III

De wijze waarop Reddy en Doraiswamy de activeringsenergie voor de oxidatie van tolueen hebben berekend, is onjuist.

K.A.Reddy en L.K.Doraiswamy
Chem. Eng. Sci. 24, 1415 (1969)

IV

Het is onwaarschijnlijk dat tijdens de reduktie van bismuth oxide bij 450°C het gevormde bismuth metaal een niet-poreuze laag vormt op het oxide-oppervlak, zoals door Massoth en Scarpiello wordt aangenomen.

F.E.Massoth en D.A.Scarpiello
J. Catal. 21, 225 (1971)

V

De wijze waarop Blakemore en Hoerl de geldigheid van hun kinetische model aantonen, is aanvechtbaar.

J.W.Blakemore en A.E.Hoerl
Chem. Eng. Progr., Symp. Ser. 42, 14 (1963)

VI

Het is wenselijk dat de bibliotheek van de TH Eindhoven de uitgave van het Bulletin voor de afdeling der Scheikundige Technologie staakt, en het aantal abonnementen op het tijdschrift Current Contents aanzienlijk uitbreidt.

VII

De bewering van Vlasov en Semavin dat bij de reduktie van UO_3 door methaan de zuurstofdiffusie door het kristalrooster niet snelheidsbepalend is, is ongegrond.

V.G.Vlasov en Yu.N.Semavin
J. Appl. Chem. USSR 40, 374
(1967)

VIII

Er zijn aanwijzigingen dat de oxidatieve dimerisatie van propeen over bismuthhoudende katalysatoren verloopt op een gereduceerd katalysatoroppervlak.

T.Seiyama, M.Egashira, T.
Sakamoto en I.Aso, J. Catal.
24, 76 (1972)

IX

Het beleid dat de nederlandse overheid voert ten aanzien van de autosport zal niet leiden tot het daarmee beoogde resultaat.

B.van Delden, Autorevue 18, 410
(1972)

X

Zolang het nog niet als onweidelijk wordt beschouwd op drijfjachten gebruik te maken van twee geweren en een loader, zijn de bezwaren tegen het vijfschots jachtgeweer ongegrond.

De Nederlandse Jager 77, 528
(1972)

J.G. Steenhof de Jong

12 december 1972.